

N67 19133

Norton Exploratory Research Division

NATIONAL RESEARCH CORPORATION

70 Memorial Drive

Cambridge, Massachusetts 02142

NRC Project No. 5116-1-01231

SUMMARY REPORT

Contract NASw-1231

MECHANISM OF THE ATMOSPHERIC INTERACTION

WITH THE FATIGUE OF METALS

August 4, 1965 to September 1, 1966

by

M.J. Hordon, M.A. Wright and M.E. Reed

Approved by:

Norman Beecher
Norman Beecher

Assistant Director
of Research

Reviewed by:

Frank J. Salomone
Frank J. Salomone

Contracts Manager

Submitted to:

Headquarters

National Aeronautics and Space Administration

400 Maryland Avenue

Washington, D.C.

ATTENTION:

Director of Space Research and Technology

Office of Advanced Research and Technology

Code RRM

FACILITY FORM 802

N67 19133

(ACCESSION NUMBER)

(THRU)

(PAGES)

(CODE)

CR-82446
(NASA CR OR TMX OR AD NUMBER)

17
(CATEGORY)

MECHANISM OF THE ATMOSPHERIC INTERACTION
WITH THE FATIGUE OF METALS

By M.J. Hordon, M.A. Wright, and M.E. Reed

Distribution of this report is provided in the interest
of information exchange. Responsibility for the contents
resides in the author or organization that prepared it.

Prepared under Contract No. NASw-1231 by ✓

NORTON EXPLORATORY RESEARCH DIVISION

NATIONAL RESEARCH CORPORATION

Cambridge, Mass.

for

NATIONAL AERONAUTICS AND SPACE ADMINISTRATION

CONTENTS

	Page
PREFACE.....	iv
SUMMARY.....	1
INTRODUCTION.....	2
EXPERIMENTAL PROCEDURES.....	3
Phase I.....	3
Apparatus and specimens.....	3
Test procedure.....	5
Phase II.....	7
Apparatus and specimens.....	7
Test procedure.....	13
EXPERIMENTAL RESULTS AND DISCUSSION.....	14
Phase I.....	14
Elevated temperature tests.....	14
Residual gas environments.....	17
Interrupted tests.....	24
Frequency tests.....	29
Metallurgical investigation.....	29
Phase II.....	41
Extreme high vacuum fatigue tests.....	41
Frequency effects.....	46
Comparison of extreme high vacuum and inter- mediate vacuum results.....	47
CONCLUSIONS.....	49
FUTURE WORK.....	50
REFERENCES.....	51

PREFACE

This is the Summary Report covering the work performed by National Research Corporation under Contract No. NASw-1231 for the Office of Advanced Research and Technology, National Aeronautics and Space Administration during the period August 4, 1965 to September 1, 1966. The program is a continuation of an investigation to examine the effect of vacuum and gas environments on the fatigue properties of metals begun under Contract No. NASw-962.

The major contributors to this program were Dr. M.A. Wright and Mr. M.E. Reed under the supervision of Dr. M.J. Hordon of the research staff of NRC. The technical monitor was Mr. R. Raring, OART, NASA, Code RRM.

Some of the results of this work were presented in the technical literature ^{1,2}.

MECHANISM OF THE ATMOSPHERIC INTERACTION
WITH THE FATIGUE OF METALS

By M.J. Hordon, M.A. Wright and M.E. Reed
National Research Corporation

SUMMARY

In a continuation of previous research on the fatigue behavior of 1100-H14 aluminum in vacuum, measurements of the fatigue properties were extended to include variations in temperature, residual gas composition and reduced pressure level. Fatigue tests both in air or vacuum interrupted after nucleation of a visible crack and continued at a different pressure level demonstrated that the crack initiation phase of the fatigue process was insensitive to the ambient gas pressure. However, the crack propagation phase was substantially retarded when the environmental pressure was below the critical transitional pressure of approximately 10^{-3} Torr noted in earlier work.

The transitional pressure level was observed to increase with both temperature and cyclic stress frequency. Fatigue tests conducted in residual atmospheres of purified O₂ and H₂O gas at intermediate pressure levels in the range 10^{-6} to 10^{-1} Torr were generally similar to the tests made at equivalent air pressures. However, tests carried out in pure H₂ gas atmosphere showed that the transition pressure level for fatigue life improvement could be raised to pressures approaching unit atmosphere. The experimental data convincingly support the oxygen absorption rate vs. crack growth rate model proposed in earlier work to account for the transition pressure effect.

With partial pressures of oxygen well below the critical level, little further improvement in the fatigue life was observed with reduced pressures down to 5×10^{-11} Torr in tests carried out in Phase II of the program. At 5×10^{-11} Torr, a two-fold increase in cyclic stress frequency resulted in a proportional increase in the number of cycles required for failure. It was concluded that the total exposure time to the residual oxygen environment was the controlling parameter for the fatigue process at this vacuum level rather than the number of alternating stress applications.

INTRODUCTION

Interest in the effect of outer space environments on the physical and mechanical properties of engineering materials has substantially increased in recent years with the growing pace of our satellite and lunar research effort. The need for more precise and extensive information on the extra terrestrial behavior of materials has developed in proportion to the expanding reliability requirements as more complex vehicles probe deeper into space for longer periods of time.

With respect to materials properties in space, the high vacuum level, estimated at 10^{-12} Torr above 2000 km height³ is of major interest. The relative absence of oxygen or water vapor molecules to react with metal surfaces as well as the likely degradation of existing adsorbed films by mechanical abrasion or cosmic erosion will strongly influence surface-sensitive properties such as fatigue.

The effects of the surrounding media on the fatigue life of metal specimens has been intensively investigated by numerous workers. It is now generally accepted that, for a given stress level, a large decrease in the number of cycles to fracture will occur if the test is conducted in a corrosive environment in contrast to conditions in vacuum. The reactive medium which surrounds the specimen usually exerts its maximum effect if it exists in the liquid state; however, the results of the original experiments performed by Gough and Sopwith⁴ demonstrate that a loss in fatigue life occurs if the test is carried out in a gaseous environment.

Fatigue tests have been carried out on a variety of metals using different environmental gas pressures. Gough and Sopwith found that the life of copper and brass could be increased if the test were carried out at an environmental pressure of 10^{-3} Torr. Further investigations showed that oxygen and water vapor had to be present to reduce the life to the normal air value.⁵ Recently, work by Snowden⁶ has indicated that the increase in fatigue life observed when lead is fatigued at progressively lower pressures occurs at a definite pressure level; the life above and below this critical point appears to be pressure independent. The effect of vacuum on the fatigue life of aluminum has been studied by Wadsworth⁷ who found that the life increased as the environmental pressure was lowered. Work by

Ham and Reichenbach⁸ produced essentially the same results. These latter authors suggested that a critical pressure level existed between 10^{-2} and 10^{-4} Torr, below which the fatigue life was substantially improved. Hordon and Reed⁹ have investigated this area in more detail in the preceding program under NASA Contract No. NASw-962 and confirmed the presence of the critical pressure level between 10^{-2} and 10^{-4} Torr; they concluded that the increase in life was due to a retardation in the crack growth rate. It has been suggested that all of the above results reflect a critical pressure dependence of monolayer oxygen or hydrogen atomic adsorption at the fatigue crack surfaces.

The following report contains a description of experiments (Phase I) performed to investigate the effects of temperature, test-interruption, and residual gas pressures on the fatigue properties of aluminum; further work is also reported (Phase II) which extends the investigation to include extremely low pressure values to less than 10^{-10} Torr.

EXPERIMENTAL PROCEDURES

Phase I

Apparatus and specimens. — The fatigue apparatus used in Phase I studies was essentially the same eight position, constant deflection unit described in previous reports under NASA Contract No. NASw-962. As shown in Figure 1, it consisted of a stainless steel circular flange on which 8 electric motor driven eccentrics were mounted. The asymmetric motion produced when the motors were activated was used to drive force rods connected through flexible bellows seals to one end of the specimen. The complete assembly was mounted on a stainless steel cylindrical chamber which could be evacuated to a pressure of 1×10^{-7} Torr. Visual observation of the specimen was possible, during stressing, through glass windows sealed to the stainless steel by Kovar fittings. It was possible to raise the environmental temperature inside the spool piece by means of a quartz covered heating element. The radiant heat from this source proved sufficient to heat the apparatus to a temperature of 100°C as measured at the specimen, by a Chromel-Alumel thermocouple.

The high purity gas used in the residual atmosphere tests was further purified by passing it through copper coils which

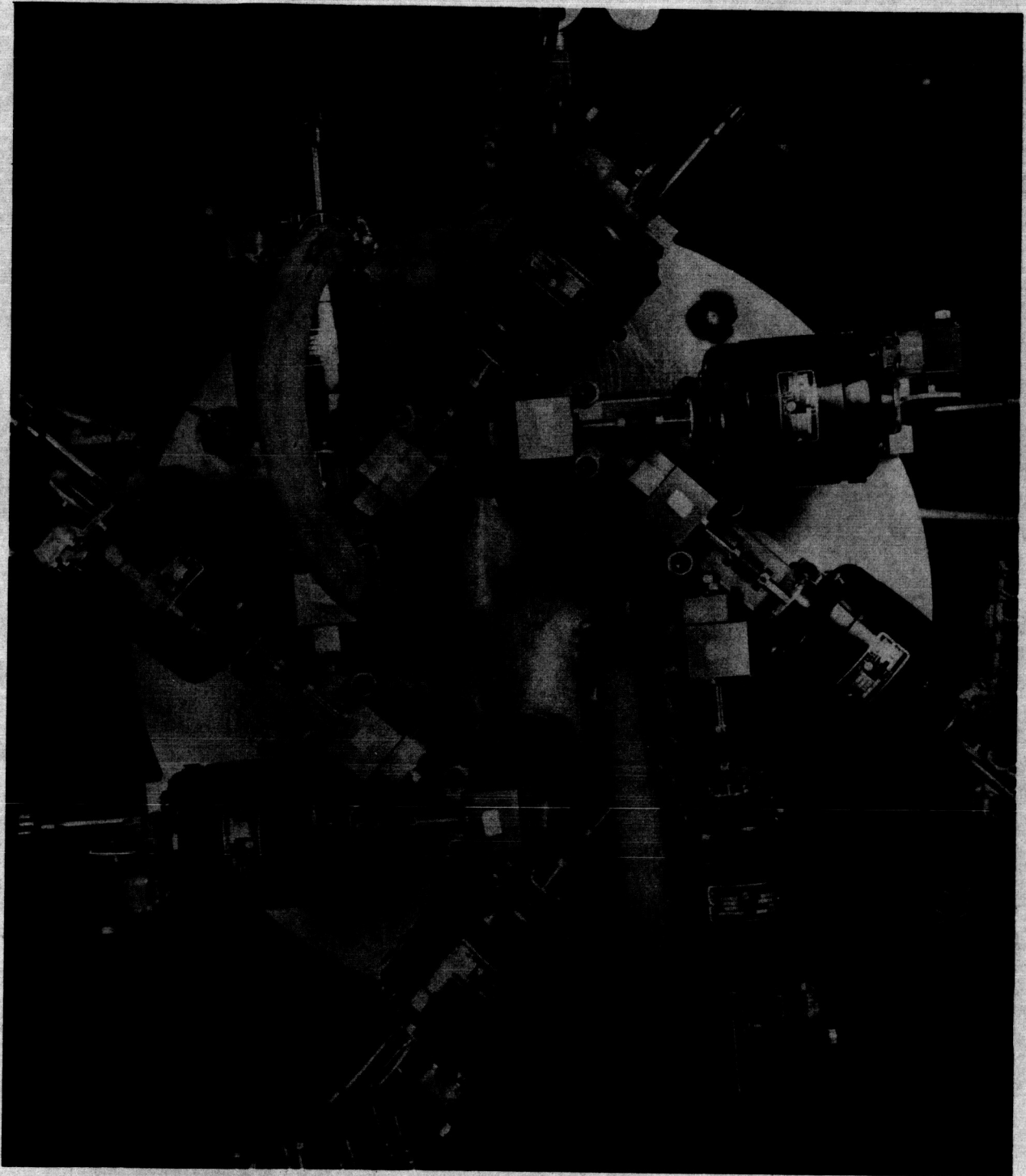


Fig. 1
TOP VIEW OF VACUUM FATIGUE APPARATUS

were maintained at a low temperature. Trace amounts of water vapor were removed from the oxygen by maintaining the coils at -100°C ; water vapor and oxygen were removed from the hydrogen by maintaining the coils at liquid nitrogen temperature, -196°C . Prior to each experiment this freeze-extraction system was evacuated, using an auxiliary mechanical pump, and refilled three times with the desired gas; the system was then allowed to stand overnight at low temperature to allow the pumping action of the low temperature region to remove any further traces of condensable impurities. The large number of turns present in a copper pipe was presumed sufficient to insure, at the low throughput rates used, the complete elimination of the condensable impurities.

For use in the fatigue testing unit, a fixed end cantilever-type specimen was selected with the dimensions shown in Figure 2. The specimen geometry was closely similar to the standard ASTM design for constant stress along the gauge length. With the aluminum samples used in the present investigation (1100-H14 Al, BHN=32), a design thickness of 0.185 in. required a force of about 20 lb to achieve the maximum bending amplitude of ± 0.040 in. The strain amplitudes in reversed bending were chosen to produce fatigue fractures in the range 5×10^4 to 10^7 cycles.

Test procedure. — Standard bend test fatigue specimens were cut and milled to shape from as received half hard aluminum sheet stock. The specimen surfaces were mechanically polished taking great care that the very fine scratches that remained in the surface after the final polishing operation were all normal to the direction of growth of the final crack. It was found from preliminary experiments that these scratches, produced by Linde 0.5 micron alumina powder, did not affect the total fatigue life.

Fatigue tests were run at selected vacuum levels according to the following procedures:

1. Specimens were selected at random and checked for dimensions.
2. After pumpdown to a stable vacuum, simultaneous fatigue tests were run at cyclic frequencies of 25 and 50 cps.
3. For each constant strain amplitude and vacuum level, four stations each were operated at the two frequencies. The

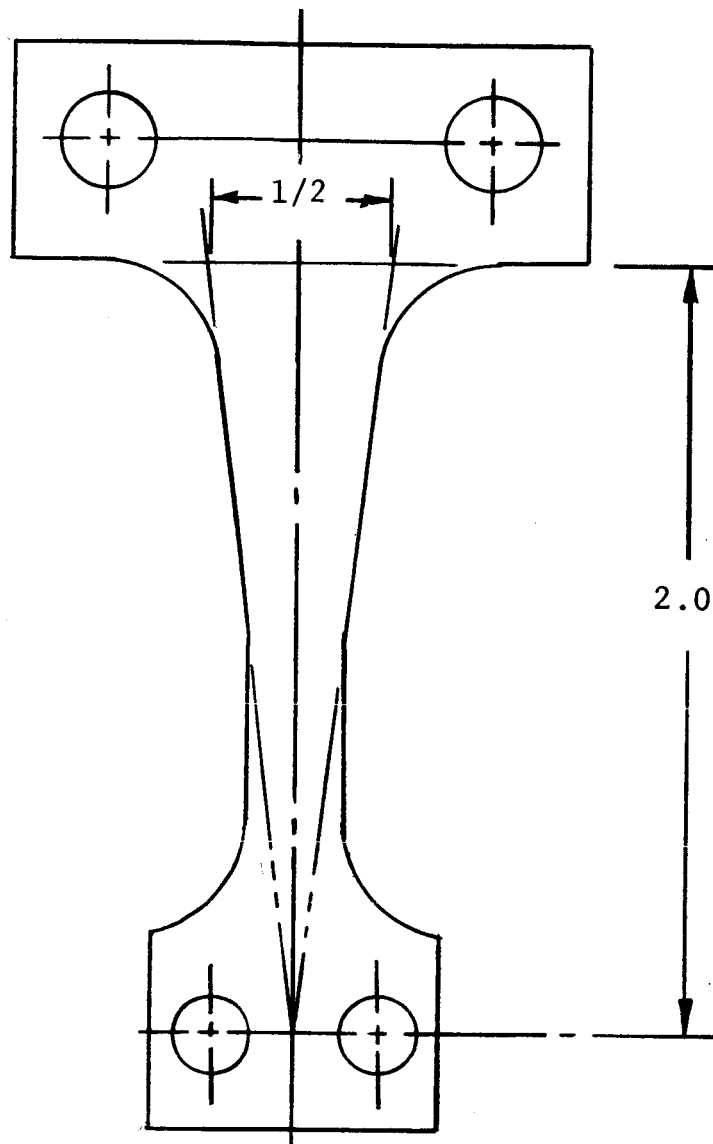


Fig. 2

PHASE I SPECIMEN OUTLINE

stations were alternated in successive pumpdowns to average the results of individual amplitudes.

4. Eight individual tests were run for each strain amplitude and frequency to obtain a high degree of confidence in the fatigue life data.

5. Additional tests were performed if excessive deviations were observed in the data.

6. During the fatigue tests, visual observations of crack formation and growth were recorded as a function of the cyclic life. Selected samples were monitored for moment force using a recorder to indicate changes in specimen mounting plate deflection.

7. The total fatigue life was taken as 100% crack extension across the sample gauge section.

Phase II

Apparatus and specimens.— As described previously ⁹, an apparatus was designed and constructed during the initial work under Contract NASw-962 to impose reverse bending loads at constant deflection at pressure levels below 10^{-9} Torr. This phase of the investigation was intended to extend observations of the effect of vacuum on fatigue properties to levels not attainable with the equipment used in Phase I studies.

The considerations underlying the design of a fatigue test device to operate at extremely low pressure levels have also been extensively described in a previous report ⁹. Basically, the unit consists of an electromagnetic vibrator which drives a central shaft. Eight specimens are concentrically mounted so that the inner ends are attached to the shaft while the outer ends are rigidly fixed to an annular base. The entire assembly was designed to be incorporated in the Extreme High Vacuum (XHV) System developed at NRC. A schematic illustration of the fatigue test assembly is shown in Figure 3. The exciter driver is in an environment of unit atmosphere with power leads and air cooling tubes extending through a cylindrical shaft to the outside. The exciter enclosure permits installation within the XHV system as shown in a general view in Figure 4.

Figure 5 is a schematic of the concentric triple bellows assembly which allows the vibrational shaft motion between the

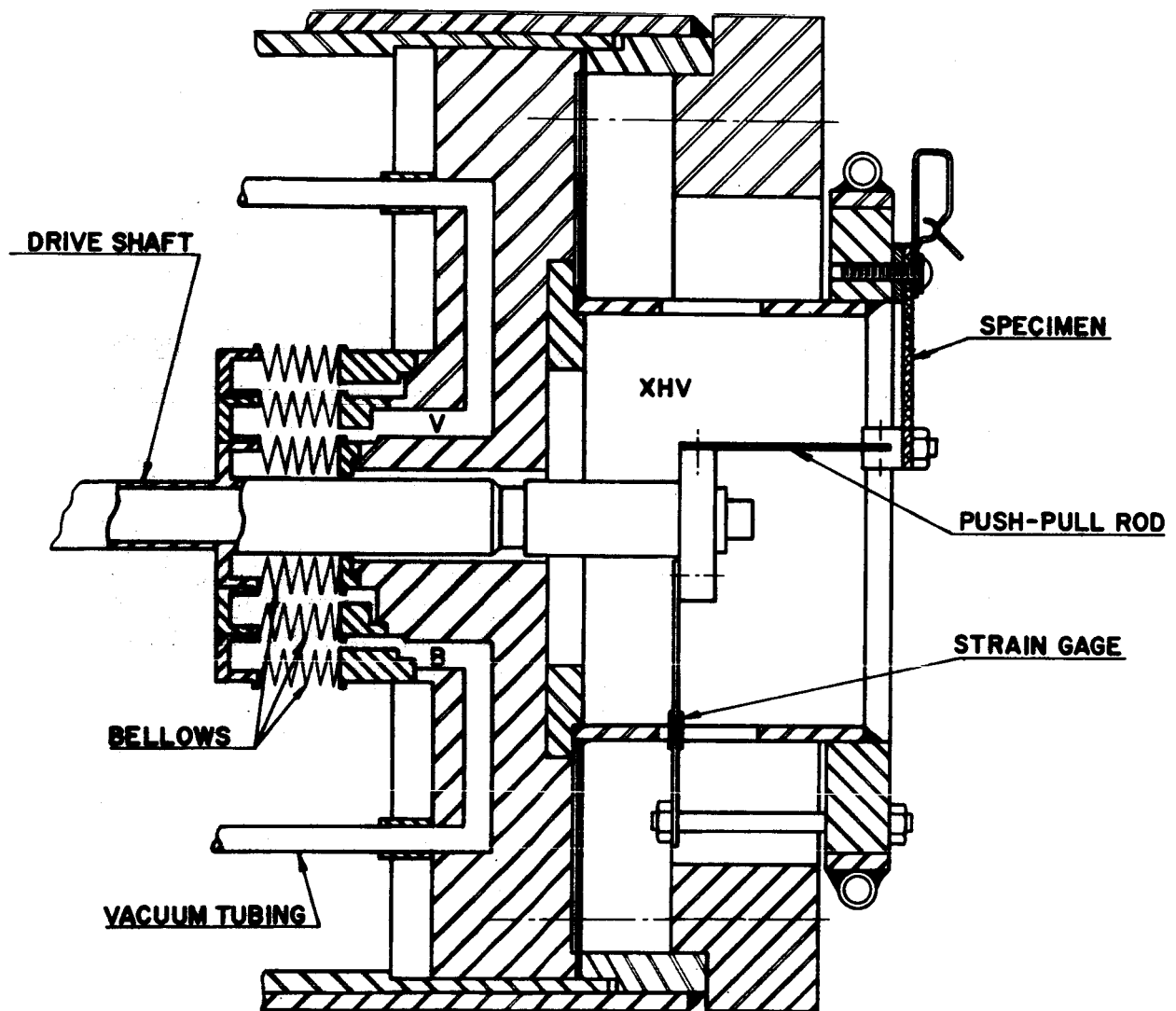


Fig. 3
FATIGUE TEST EXCITER AND ENCLOSURE

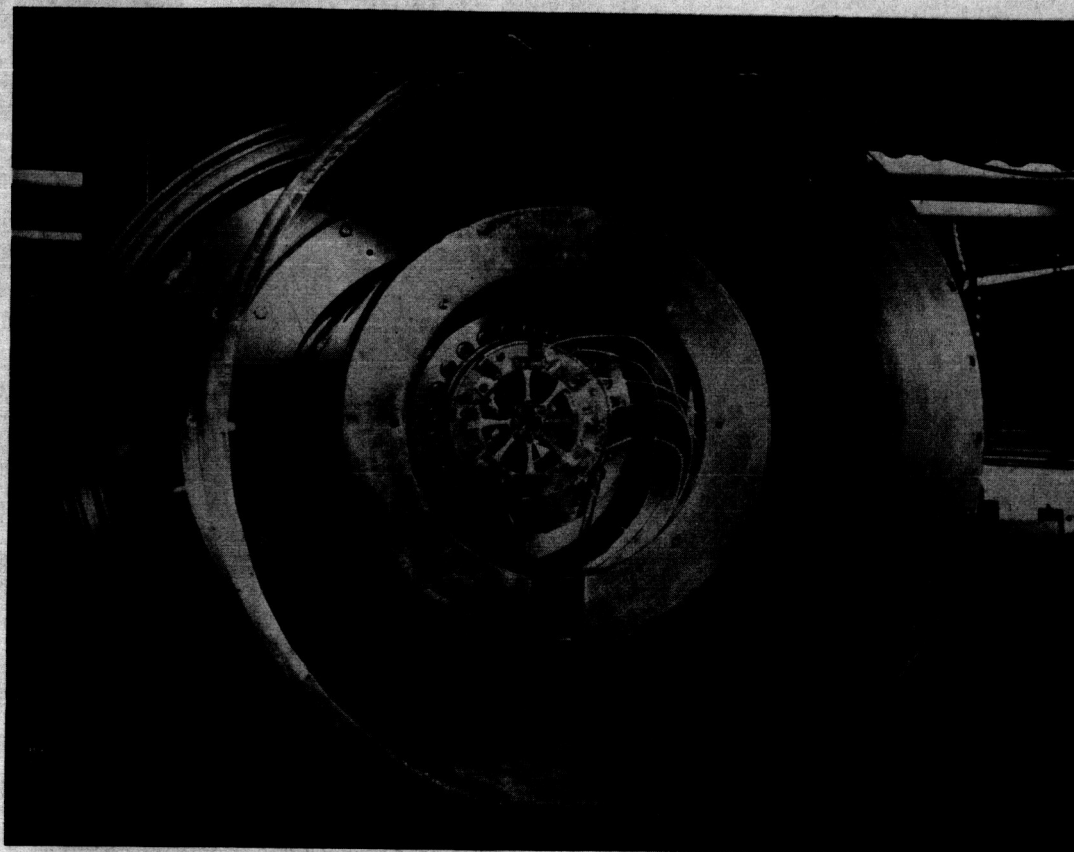


Fig. 4
INSTALLATION OF FATIGUE TEST APPARATUS
IN XHV SYSTEM

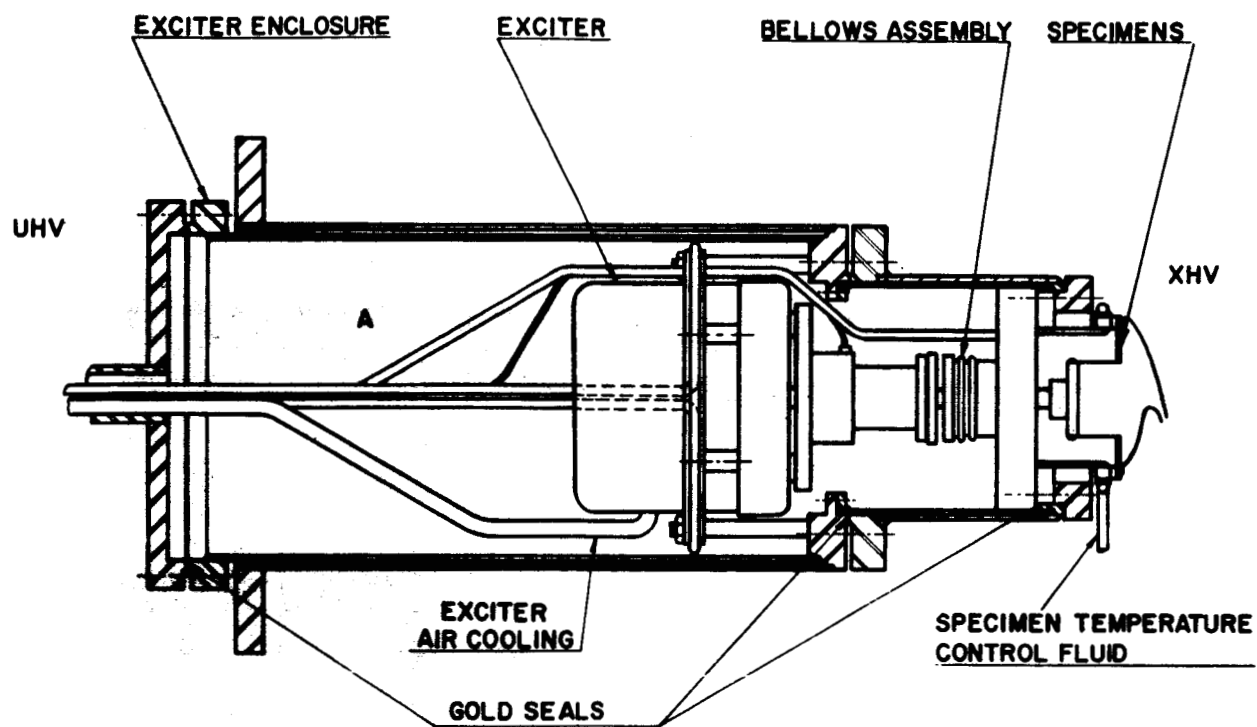


Fig. 5
 SCHEMATIC OF FATIGUE TEST ASSEMBLY
 WITH BELLOWS

atmospheric pressure region of the enclosure and the XHV region without introducing a heavy gas load into the vacuum area. Three gold seals were used in place of elastomeric gaskets to seal the exciter enclosure. The annuli between the bellows are separately pumped through tubing extending out through the main exciter access shaft. The outer annulus labelled "B" in Figure 5 was used to balance the bellows position prior to system pumpdown. The inner annulus labelled "V" was evacuated to approximately 10^{-6} Torr. Any small leak in the inner bellows then would not seriously compromise the high vacuum working volume. The triple bellows design prevents any catastrophic bellows failure.

The moving drive shaft which extends through the center of the bellows assembly is connected to the specimens through 8 columnar push-pull rods, outlined in Figure 5. The specimens were rigidly clamped to the face of a vertically faced flange. All 8 specimens move simultaneously in bending as the shaft is displaced.

The specimens with a 1.0 in. gauge length by 0.080 in. in thickness, were made from 1100-H14 aluminum sheet and were shaped as shown in Figure 6. Silicon carbide paper No. 600A was used to wet polish the surfaces.

The specimens are exposed to the vacuum created by the helium cooled copper cylinder shown in Figure 4. However, a liquid nitrogen cooled thermal shield is interposed between the warm specimens and the helium cooled cylinder to reduce the heat load to the helium refrigerator. This thermal shield is a double walled optical baffle with holes spaced to allow non-condensable gas removal by diffusion pumping.

A Redhead magnetron gauge operated from an NRC Equipment Corporation Model 752 gauge control is mounted with the gauge envelope opening directly facing the specimens. In this way, the gauge responds to gas emitted from the specimens and senses the molecular number density surrounding the specimens.

The heart of the vibrating system, the vibration exciter, is a permanent magnet, moving coil type of vibration generator manufactured by Pye-Ling Ltd. The model V50 mk 1 has a nominal 50 lb rating in the 20 to 100 cps frequency range and is air cooled.

Power for driving the exciter originates in an audio frequency sine wave generator. This is amplified by a high fidel-



Fig. 6

DETAIL OF FATIGUE TEST APPARATUS SHOWING SPECIMEN ASSEMBLY

ity power amplifier and is connected directly to the vibration generator.

Amplitude control is achieved with a strain gauge circuit providing variable gain between the signal generator and the amplifier. Ceramic bonded strain gauges are mounted on flat stainless steel spring stock so that the spring stock is deflected with the same amplitude as the specimens. A very slight decrease in specimen amplitude due to changes in material properties causes a compensating decrease in the variable gain stage. With this system, deflection amplitude can be held to ± 0.001 in.

Test procedure. — Median fatigue life S-N curves were obtained in atmospheric air and in extremely high vacuums after initial stress-strain calibration tests were made on the specimens and after calibration of the electronic excitation power system. The stress-strain calibrations were made by rigidly mounting the large end of a test specimen on a test block bolted to an Instron Model TT-C testing machine. The small end of the specimen was then deflected by pulling it with a flat steel ribbon clamped at one end in the machine.

Tight clamping of the specimen was found to be critical and it was necessary to use a clamping plate over the specimen. The clamping plate used in these tests and in the vibration fatigue tests was $1/8$ in. thick and the same width and breadth as the large end of the specimens. The length of the steel ribbon was found to affect the force-deflection slope also. With tight clamping and steel ribbon approximately two inches long, values of the elastic modulus E were obtained which agreed well with other published values.¹⁰

The equation

$$F/y = E b h^3 / 6 L^3 \quad (1)$$

was used to establish the value of E, where F is the deflecting force measured on the Instron machine, y is the deflection, b is the effective width of the specimen at the clamped base, h is the thickness of the specimen, and L is the length of the specimen between the clamped edge and the center line of the deflecting force.

Values of stress at the surface of the specimen in the triangular stress area were then given by the equation

$$S = h E y / L^2 \quad (2)$$

where S is the bending stress in psi.

After completion of the stress-strain calibration, the electrical circuit calibrations were made. These consisted of obtaining voltage measurements from the strain gauge circuit under dynamic conditions while visually measuring the amplitude of the specimen vibration. The calibration has to be made at each frequency to be used since the response of the capacitive circuit elements varies with frequency. A telescope with a filar eyepiece was used to view the vibrating specimen. A stroboscope was used to illuminate the specimen so that the ends of the stroke could be viewed in the telescope for measurement. The stroboscope also served as the frequency standard.

The eight test specimens, after ultrasonically cleaning them in acetone and then in pure grain alcohol, were radially arranged on the mounting flange for each group test. The specimens were then vibrated at the desired amplitude and frequency. During air tests it was possible to check the amplitude visually as well as to monitor the amplitude voltage indication. As each specimen failed, it separated due to the light spring action of the push-pull rods and electrically opened the circuit to a clock timer thus enabling accurate determination of cycles to failure.

Median fatigue life S-N curves were determined from the results of tests on five groups of eight specimens in vacuum and from six groups of eight specimens in air. All tests were made at or near room temperature. All tests were run at 100 cps except that one group was run at 200 cps to compare with the 100cps test at one stress amplitude.

EXPERIMENTAL RESULTS AND DISCUSSION

Phase I

Elevated temperature tests. — Measurements of the fracture life in reverse bending fatigue for aluminum were made at 20° and 100°C with a constant surface strain amplitude of + 0.0012 in./in. corresponding to a maximum bend stress of about 12,000 psi for the specimens tested. Fatigue tests were conducted at pressure levels varying from unit atmosphere to 2×10^{-7} Torr at cyclic frequencies of 25 and 50 cps to vary the time rate of crack extension.

The effect of a decrease in pressure on the fatigue life of aluminum at these different temperatures is shown in Figure 7. It can be seen that a critical pressure exists in the range

10^{-2} to 10^{-3} Torr above and below which little fatigue life dependence is observed. It is evident that in comparison to the room temperature results, a well defined increase in the critical pressure required for fatigue improvement resulted from the increase in the operating temperature.

The critical pressure required for crack growth retardation can be estimated from the pressure dependence of the rate of oxygen absorption at the crack tip (v_a) and the observed time rate of crack propagation (v_c)^{1,2,9}. The linear rate of absorption (v_a) for a monolayer of oxygen adatoms per unit area of exposed crack surface can be derived:¹¹

$$v_a = l/t_a = K p_{O_2}/(MT)^{1/2} \quad (3)$$

where

$$K = \frac{3.5 \times 10^{22} \text{ } l/A}{3/8 (l/r)^2} \quad (4)$$

and K is a geometrical factor to account for the molecular arrival rate at the base of a long, narrow crack of length l and width r ; A is the cross-sectional area, and M the molecular weight of the adatom, p_{O_2} is the residual partial pressure of oxygen and T is the absolute temperature.

The transition pressure for fatigue crack retardation may be interpreted as the reduced pressure for which $v_a = v_c$ ⁹. At higher pressures, v_a will be greater than v_c and the crack front will be continuously saturated with O_2 ; at lower pressures, v_c will be greater than v_a and the crack surfaces will not acquire an adsorbed film. For aluminum, a comparison of the variation of v_a for oxygen at room temperature and v_c with pressure for the initial 10 percent of crack extension, shows that the two rates were equivalent at about 10^{-3} Torr in agreement with the well-defined change in the fatigue life found in this pressure range.

On the basis of this competing rate mechanism, the effect of temperature shown in Figure 7 on the transition pressure may be inferred;

$$\frac{v_{a2}}{v_{a1}} = \left(\frac{T_1}{T_2} \right)^{1/2} \quad (5)$$

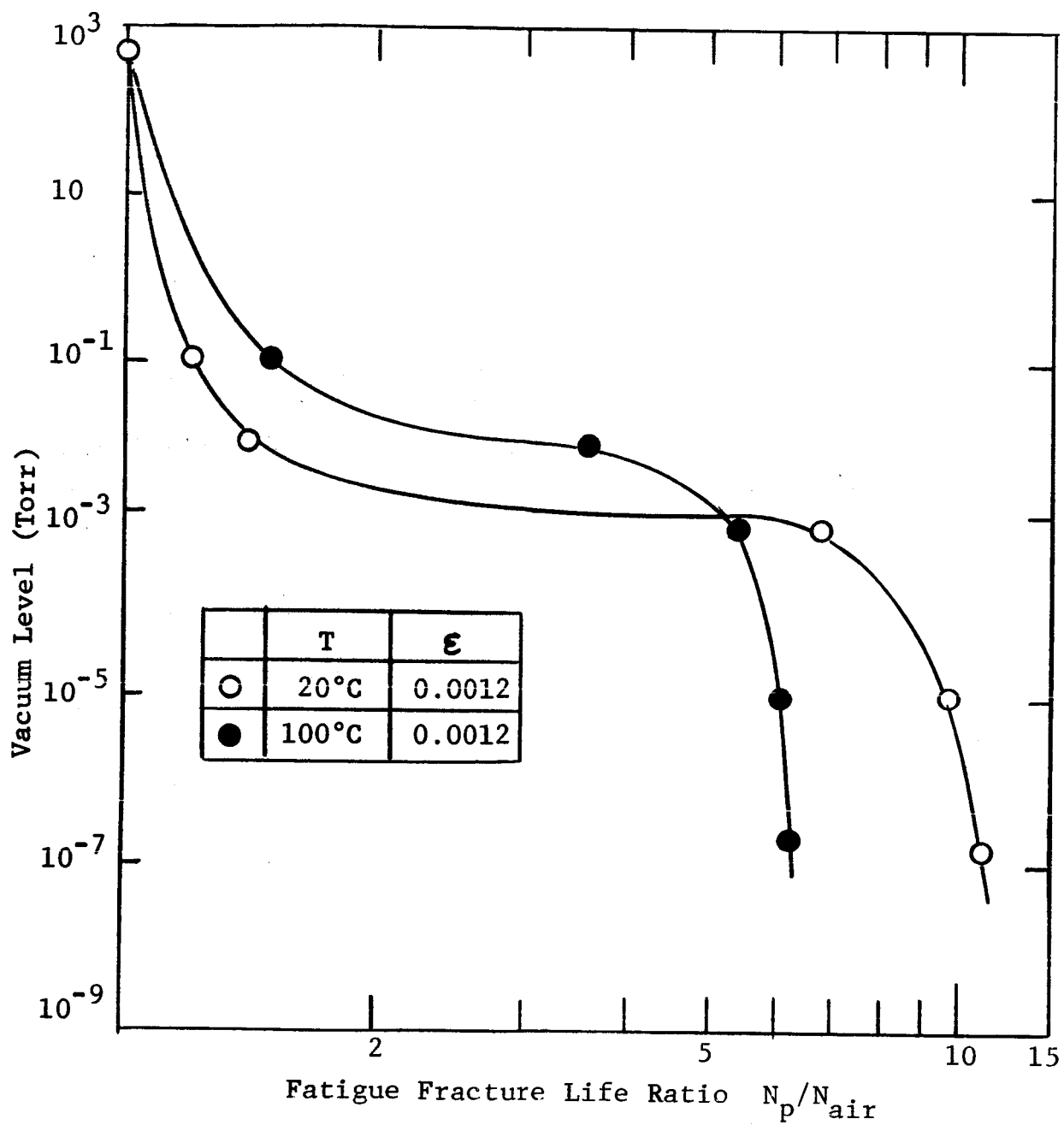


Fig. 7

PRESSURE DEPENDENCE OF THE FATIGUE FRACTURE LIFE COMPARED
TO STANDARD ATMOSPHERE DATA AT 20°C AND 100°C

Taking $T_1 = 291^\circ\text{K}$ and $T_2 = 373^\circ\text{K}$, $v_a(100^\circ\text{C}) = 0.88 v_a(20^\circ\text{C})$. The shift in v_a with temperature is illustrated in Figure 8. The major portion of the transition pressure increase can be accounted for by a significant increase in the observed fatigue crack growth rate v_c . As shown in Figure 8 measurements of the average propagation rate for the initial 10 percent of crack extension gave a value of $v_c(100^\circ\text{C})$ about equal to 4 to 5 times $v_c(20^\circ\text{C})$ through the entire vacuum range tested. The increase in the growth rate with temperature is consistent with the decrease in fatigue life generally observed for pure metals with rise in temperature.¹²

The combined effect of the changes in the linear adsorption and propagation rates was to shift the pressure level at which the rates are equal from approximately 2×10^{-3} Torr to 10^{-2} Torr as indicated in Figure 8. The increase in the critical pressure for fatigue enhancement shown in Figure 7 was in close agreement with this derived pressure change.

Residual gas environments. — It has been shown that a discontinuous decrease in fatigue life occurs as the environmental pressure of the test specimen is raised from 10^{-7} Torr to atmosphere. This decrease in fatigue life has been attributed generally to the action of oxygen in the vicinity of the fatigue crack. The proposed mechanism is the association and adsorption of oxygen molecules on the freshly formed cracked surfaces to form, presumably, a metal oxide. This material inhibits the reversal of slip along the fatigue glide bands and prevents rewelding of the cracks.

In the case of aluminum, a second mechanism comprising the dissociation of water vapor molecules and subsequent adsorption of hydrogen (H^+) ions on the crack surfaces has been advanced in order to explain the accelerated effect of water vapor in the atmosphere in promotion of crack formation and growth. Since aluminum is a reactive metal, it is likely that both mechanisms may operate during fatigue stressing.

Fatigue tests were carried out using residual gas pressures of oxygen, water vapor and hydrogen. Great care was taken to eliminate all trace impurities from these gases by passing them through the freeze extraction apparatus. All tests were run dynamically by allowing a small steady stream of the required gas to pass through the system while the pumps were still operating. The environmental pressure level could be accurately maintained by adjusting the rate of input of the gas.

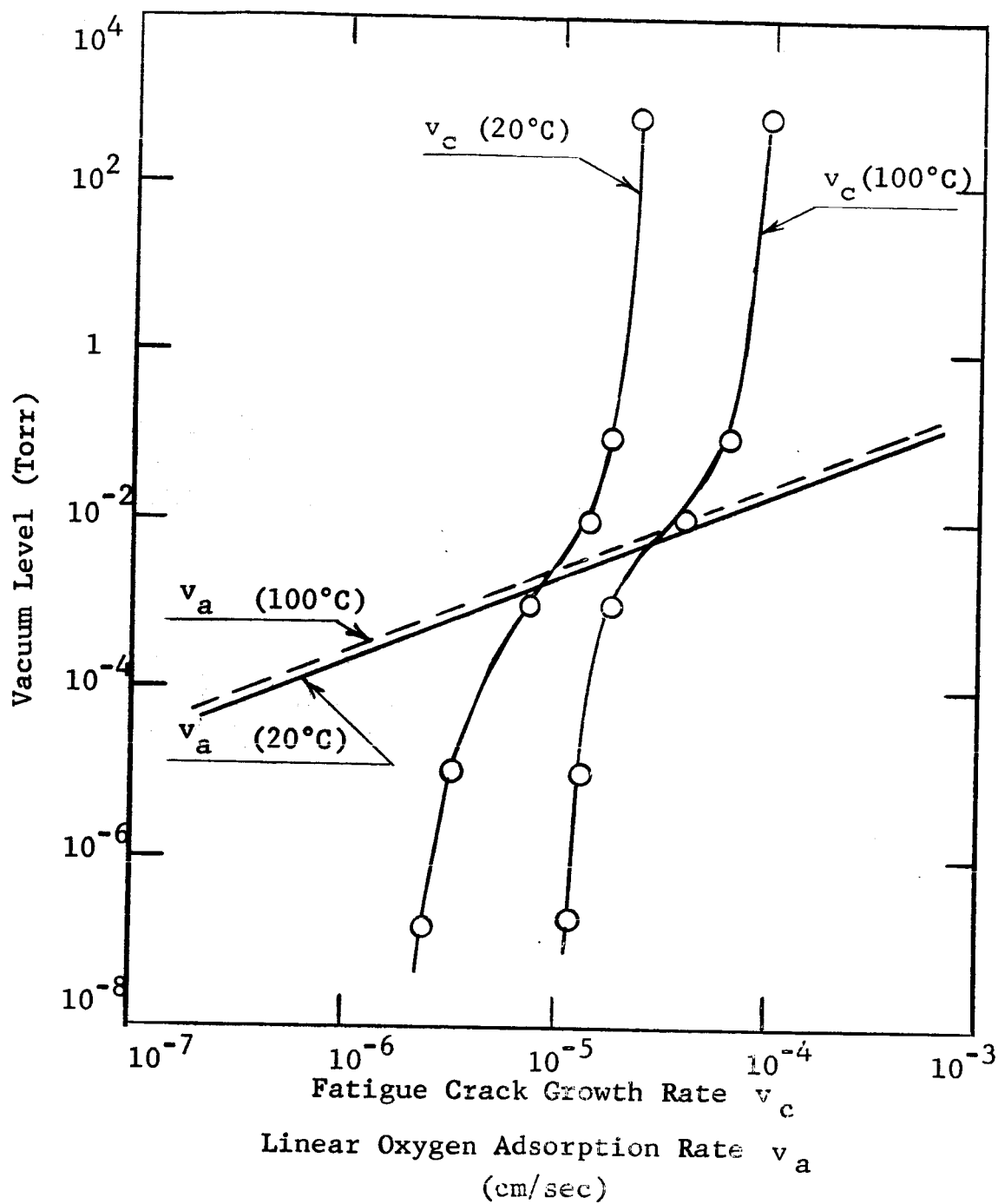


Fig. 8

VARIATION OF THE MEASURED CRACK GROWTH RATE v_c AND THE CALCULATED LINEAR ADSORPTION RATE v_a WITH PRESSURE AT

18 20°C AND 100°C.

The ambient pressure levels were obtained using the purest materials available; 99.9 percent pure oxygen was supplied by the Linde Division of Union Carbide; 99.999 percent pure hydrogen was obtained from the J.T. Baker Company; the water vapor experiments were conducted using triple distilled material.

The effects of the residual pressures of the various gases on the fatigue life of aluminum are shown in Tables I through V. A graphical representation of the low stress data is shown in Figure 9. The results were statistically analyzed using Student's "t" test ¹³ and it was found that the results for oxygen and water were identical; a large increase in fatigue life was observed at the same critical pressure level. It can easily be seen that above and below this value little dependence of fatigue life with pressure was observed.

The results obtained when hydrogen was used to provide the residual gas pressure are significantly different from those discussed above. It is apparent that the fatigue life in hydrogen is independent of the pressure of the gas and is identical, at all levels, to the lives obtained using a low pressure environment composed of either air, oxygen, or water vapor. This behavior suggests that the mechanism of fatigue crack retardation was not dependent on a hydrogen-metal reaction but was rather the result of an absence of reactive oxygen molecules in the gas. It is reasoned therefore that the apparent increase in transition pressure actually results from a "blanketing" effect; the hydrogen gas does not contain a high enough concentration of reactive impurities to effect the crack growth rate.

The effect of the various gaseous media on the crack propagation rate is indicated in Figure 10. It can be seen that the number of cycles of stress necessary to form a crack of a given length is only dependent on the pressure and does not depend on the environmental composition. The crack propagation rate data obtained using hydrogen gas are, as would be expected, independent of pressure and correspond to the results obtained from specimens fatigued in high vacuum. The damaging effect of water vapor or oxygen on the fatigue life of aluminum is readily apparent.

It may be inferred that oxygen or water vapor are, presumably, also responsible for the decrease in life observed when aluminum is stressed in a laboratory air environment. It was not detected in the present experiments, whether water vapor in the molecular state is responsible for the large change in crack growth rate or whether catalytic decomposition at the

TABLE I
THE EFFECT OF OXYGEN PRESSURE ON FATIGUE LIFE
STRESS LEVEL = 11.4×10^3 psi

Pressure (Torr)	No. of Specimens	50 cps		25 cps	
		Mean	Std. dev.	Mean	Std. dev.
10^{-1}	6	1.26	0.26	0.91	0.16
10^{-2}	6	1.50	0.25	1.11	0.07
10^{-5}	6	2.68	0.49	2.39	0.08
10^{-6}	6	2.14	0.33	1.98	0.22

TABLE II
THE EFFECT OF OXYGEN PRESSURE ON FATIGUE LIFE
STRESS LEVEL = 18.2×10^3 psi

Pressure (Torr)	No. of Specimens	50 cps		25 cps	
		Mean	Std. dev.	Mean	Std. dev.
10^{-1}	6	-	-	-	-
10^{-2}	6	0.097	-	0.099	-
10^{-5}	6	0.169	0.008	0.151	0.158
10^{-6}	6	0.177	0.009	0.012	0.029

TABLE III
THE EFFECT OF WATER VAPOR PRESSURE ON FATIGUE LIFE
STRESS LEVEL = 11.4×10^3 psi

Pressure (Torr)	No. of Specimens	50 cps		25 cps	
		Mean	Std. dev.	Mean	Std. dev.
1	6	0.68	0.066	0.56	0.06
10^{-1}	6	0.75	0.039	0.62	0.11
10^{-2}	6	1.75	0.22	1.12	0.24
10^{-5}	6	2.80	0.69	2.64	0.64
10^{-6}	6	2.42	0.61	2.12	0.49

TABLE IV
THE EFFECT OF WATER VAPOR PRESSURE ON FATIGUE LIFE
STRESS LEVEL = 18.2×10^3 psi

Pressure (Torr)	No. of Specimens	50 cps		25 cps	
		Mean	Std. dev.	Mean	Std. dev.
1	6	-	-	-	-
10^{-1}	6	-	-	-	-
10^{-2}	6	0.077	0.015	0.071	0.053
10^{-5}	6	0.186	0.009	0.187	0.023
10^{-6}	6	0.165	0.010	0.178	0.026

TABLE V
EFFECT OF HYDROGEN PRESSURE ON FATIGUE LIFE
STRESS LEVEL = 11.4×10^3 psi

Pressure (Torr)	No. of Specimens	50 cps		25 cps	
		Mean	Std. dev.	Mean	Std. dev.
2×10^{-1}	6	2.42	0.061	2.12	0.43
2×10^{-2}	6	2.32	0.39	2.12	0.39
2×10^{-5}	6	2.062	0.37	2.11	0.09
2×10^{-6}	6	2.105	0.31	2.21	0.17

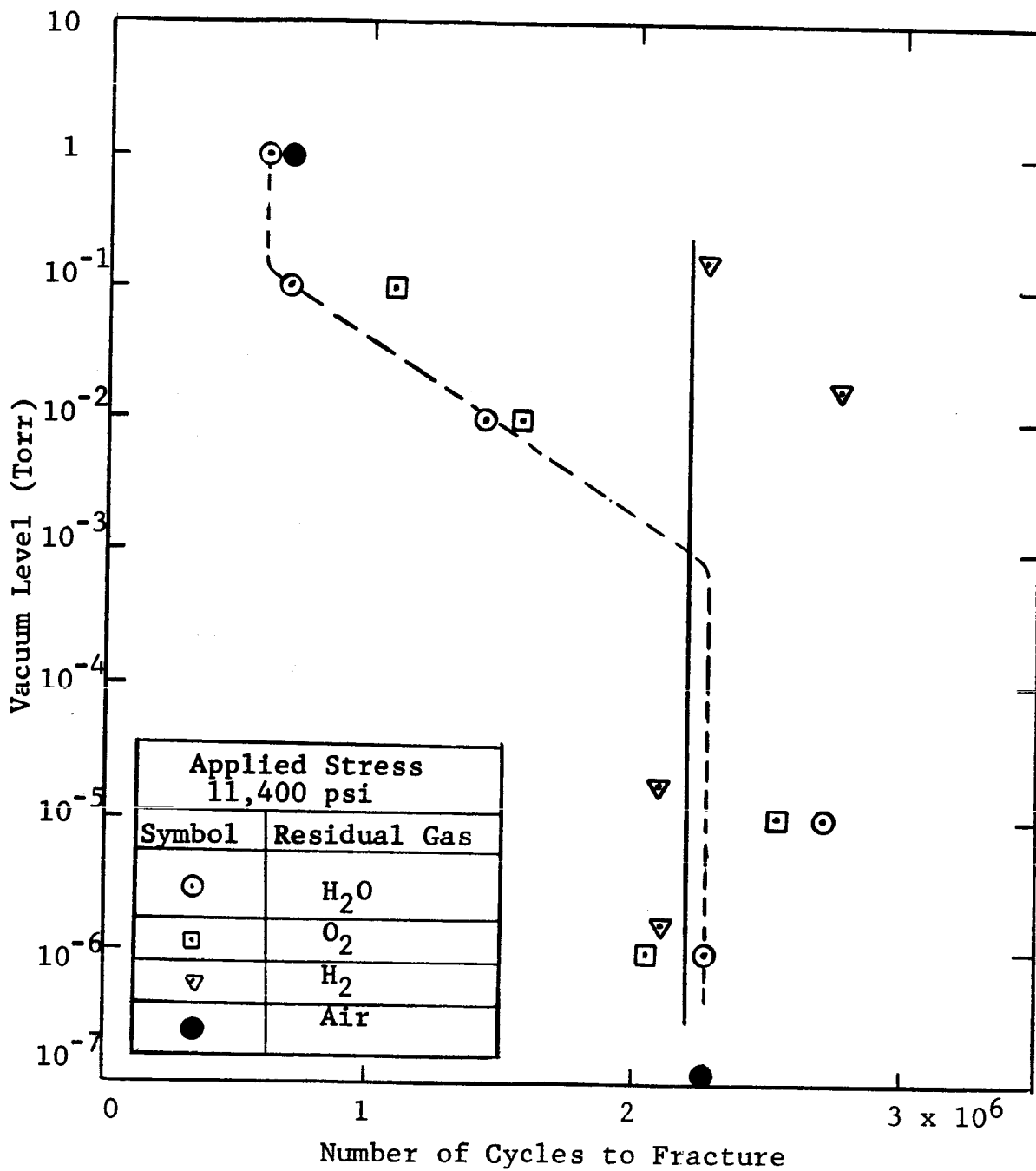


Fig. 9

VARIATION OF THE FATIGUE LIFE WITH RESIDUAL GAS PRESSURES

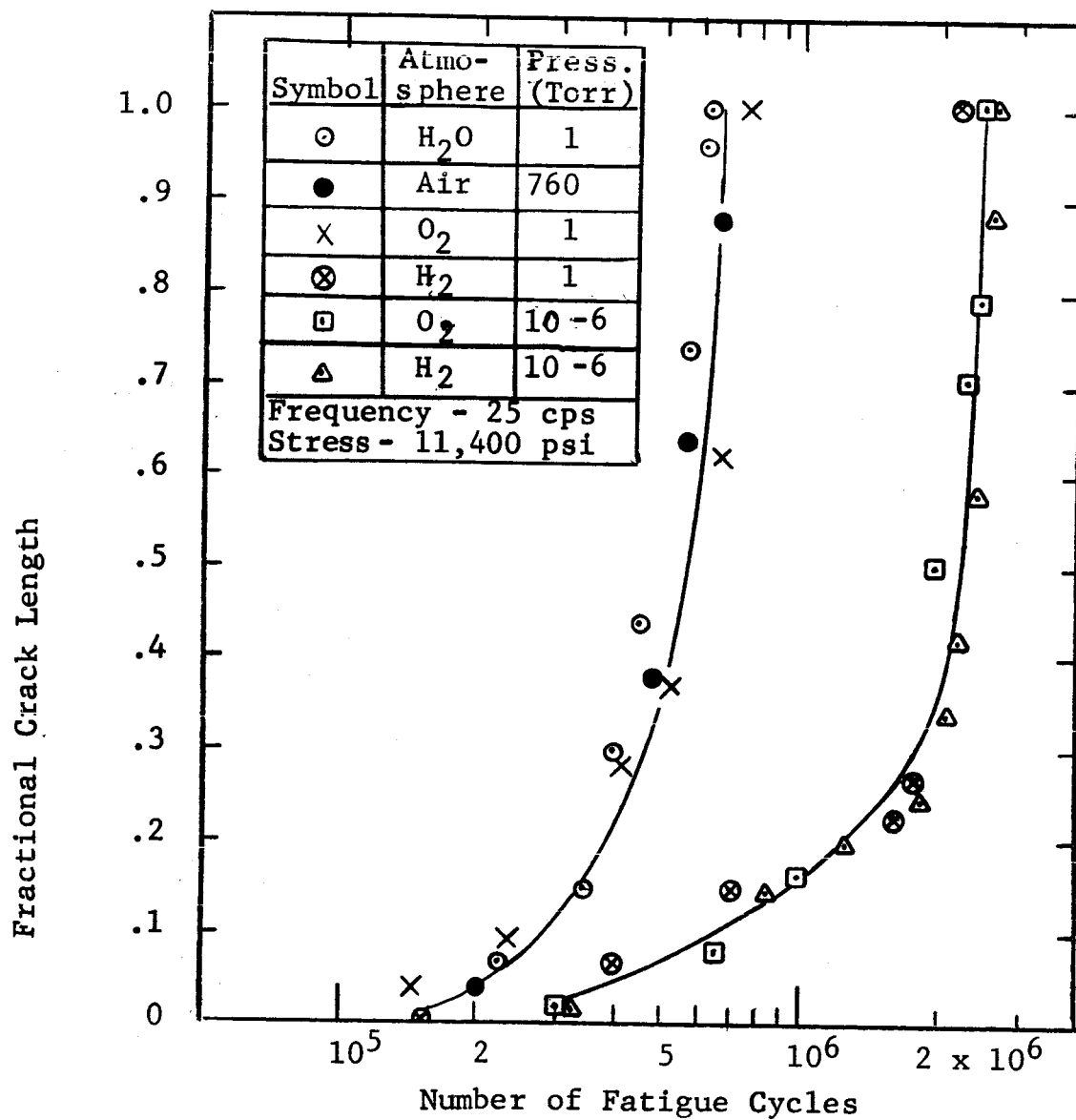


Fig. 10

THE EFFECT OF RESIDUAL GAS PRESSURES
ON CRACK PROPAGATION

aluminum metal surface produced oxygen in local quantities sufficient to effect the fatigue life. The actual concentration of oxygen necessary to increase the rate of crack propagation can be calculated from the formula:

$$M = 9.656 \times 10^{18} P/T \quad (6)$$

where M is number of molecules O₂/cc, P is critical pressure in Torr and T is the absolute temperature. For P = 10⁻³ Torr and T = 300°K, then N = 3.22 x 10¹³ molecules O₂/cc.

The hydrogen used in this investigation had an impurity content of 0.001%. It can be calculated that at a pressure of 10⁻³ Torr the maximum concentration of oxygen in the fatigue system could only have been 3.22 x 10⁸ molecules/cc; this proved insufficient to effect the total fatigue life. It is interesting to note that the estimated critical transition pressure for hydrogen, and indeed for any supposedly inert gas, of this purity, is 100 Torr.

Interrupted tests. — The fatigue process can generally be separated into two major components: Stage 1, comprising that portion of the fatigue life required to nucleate or initiate a dominant crack, and Stage 2, the number of stress cycles to propagate the crack through the specimen to final fracture. In the present investigation, the effect of pressure on the two stages was studied by initiating a crack at one pressure level and propagating it at another.

The first series of tests consisted of initiating a crack at 10⁻⁷ Torr and then propagating it at atmospheric pressure (7.6 x 10² Torr). The second series consisted of initiating the crack in air and propagating it in the lower pressure environment. Typical propagation curves are shown in Figures 11 and 12. It can be seen that a specimen subjected to a given crack propagation environment will exhibit a slightly longer fatigue life if the disastrous fatigue crack is initiated in vacuum. At low stress levels the specimen that has been initially subjected to a fatigue stress in vacuum exhibits a life 50 percent greater than the specimen fatigued to fracture completely in air. Conversely, a specimen that has a fatigue crack nucleated in air, will exhibit a life 12 percent smaller than a specimen fatigued to fracture completely in vacuum.

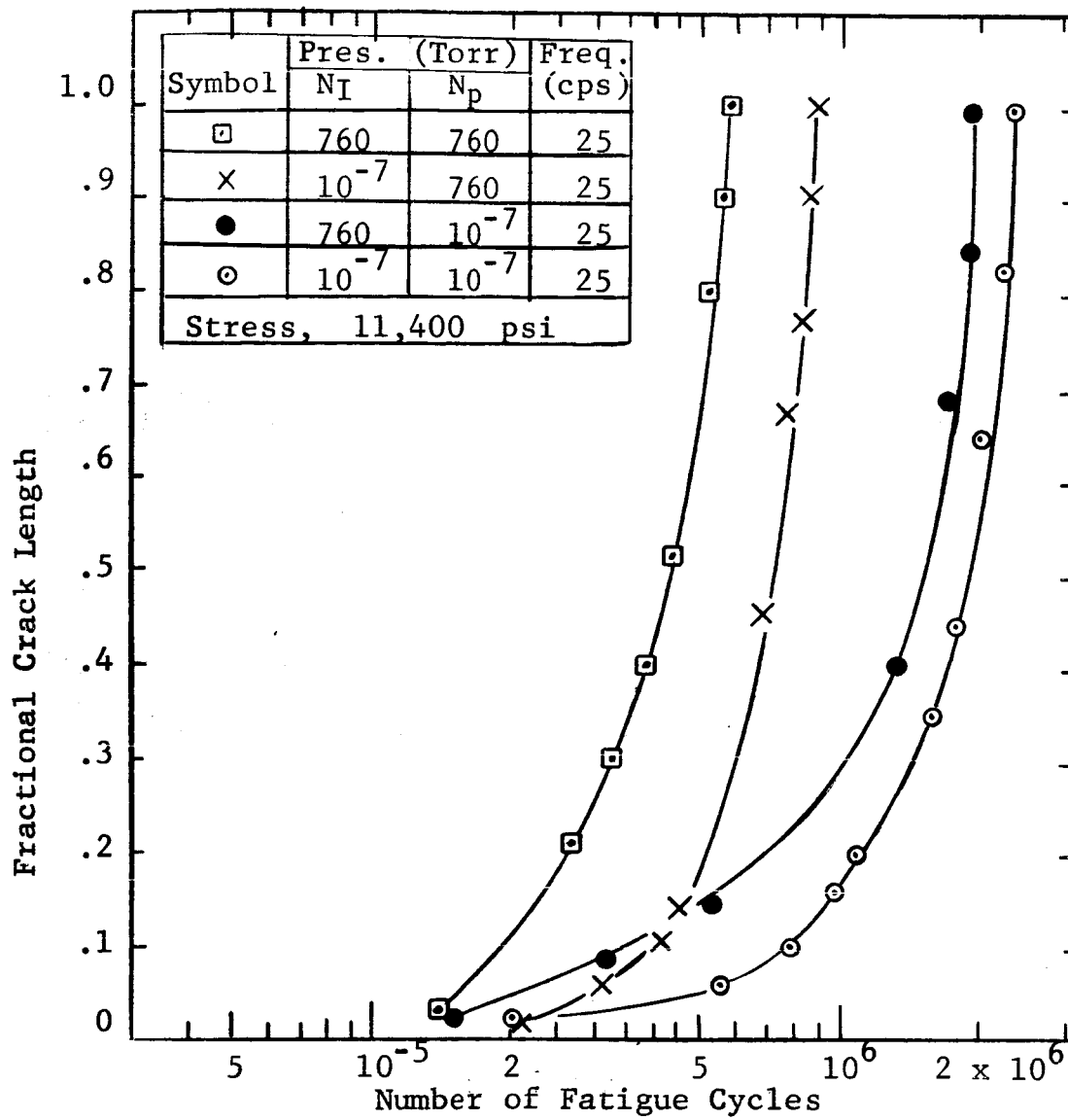


Fig. 11

THE EFFECT OF TEST INTERRUPTION ON CRACK
PROPAGATION AT 11,400 PSI

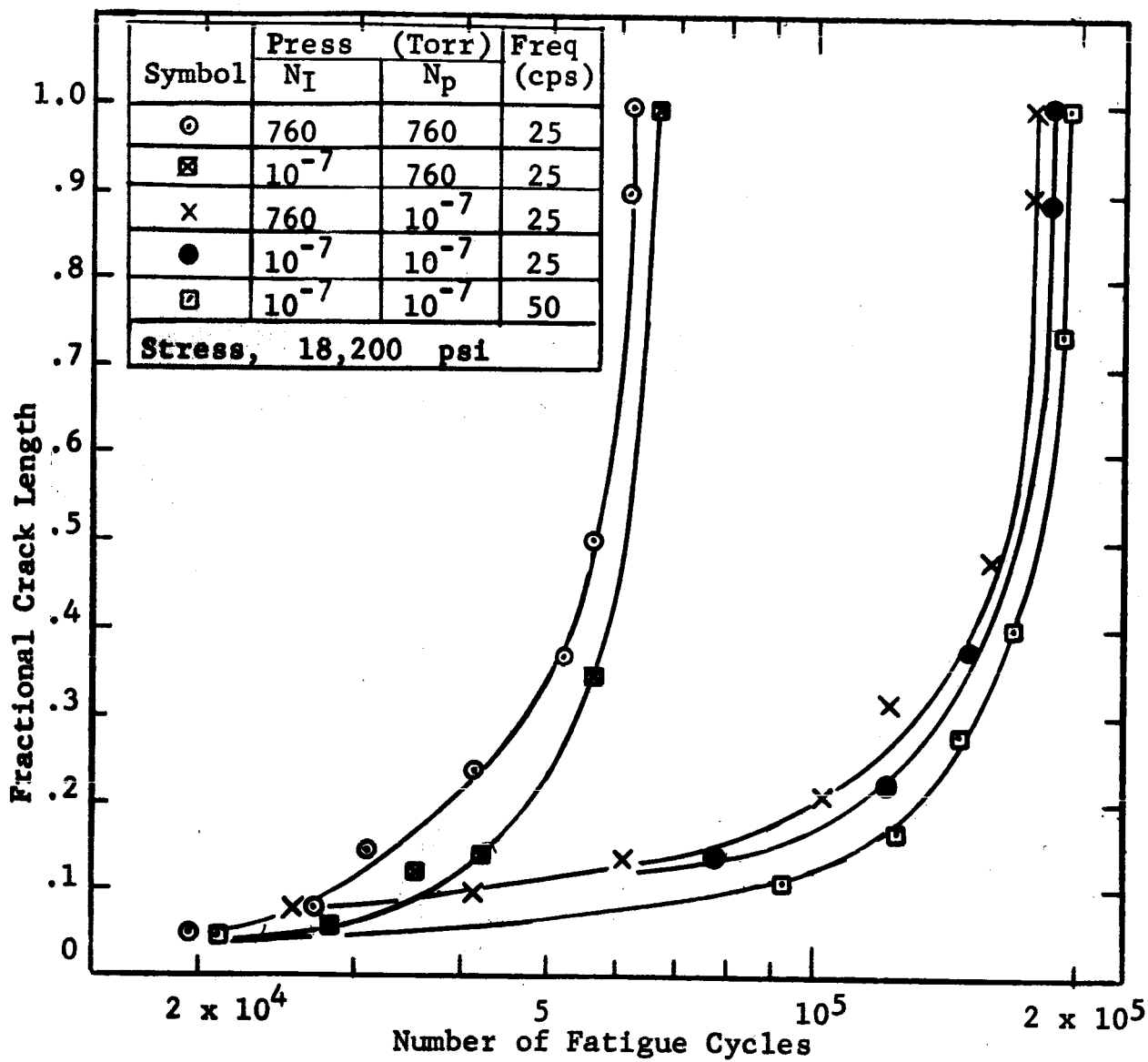


Fig. 12

THE EFFECT OF TEST INTERRUPTION ON
CRACK PROPAGATION AT 18,200 PSI.

Figure 13 illustrates the relationship between the crack growth rate and the actual crack length observed for the two pressure levels, 10^{-7} Torr and 7.6×10^2 Torr. It can be seen that a generally constant difference in propagation rate exists for the two pressure levels; the numerical value of this difference is 5, thus

$$\frac{d\ell}{dN} \text{ (atm)} \approx 5 \frac{d\ell}{dN} \text{ (vac)} \quad (7)$$

The crack nucleation time N_I is relatively unaffected by the atmosphere in which the fatigue test is conducted, thus the number of cycles of stress to form a crack of a given length in air, N_A^* , can be described by the expression:

$$N_A^* = N_I + N_{PA} \quad (8)$$

where N_{PA} is the number of cycles to propagate the initial crack nucleus to a given length in air.

From Equation (7);

$$5 N_{PA} = N_{PV} \quad (9)$$

where N_{PV} is the number of cycles to propagate the initial crack nucleus to the given length in vacuum. It can readily be seen therefore that the number of cycles to form a crack of a given length in vacuum (N_V^*) can be described by

$$N_V^* = N_I + 5 N_{PA} \quad (10)$$

Combining Equations (8) and (10):

$$N_I = \left(5 N_A^* - N_V^* \right) / 4 \quad (11)$$

For the fatigue tests in the present work run at constant surface strain amplitudes of $\pm 1.2 \times 10^{-3}$ in/in., representative values for N_A^* and N_V^* to propagate a crack 10^{-2} cm in length were

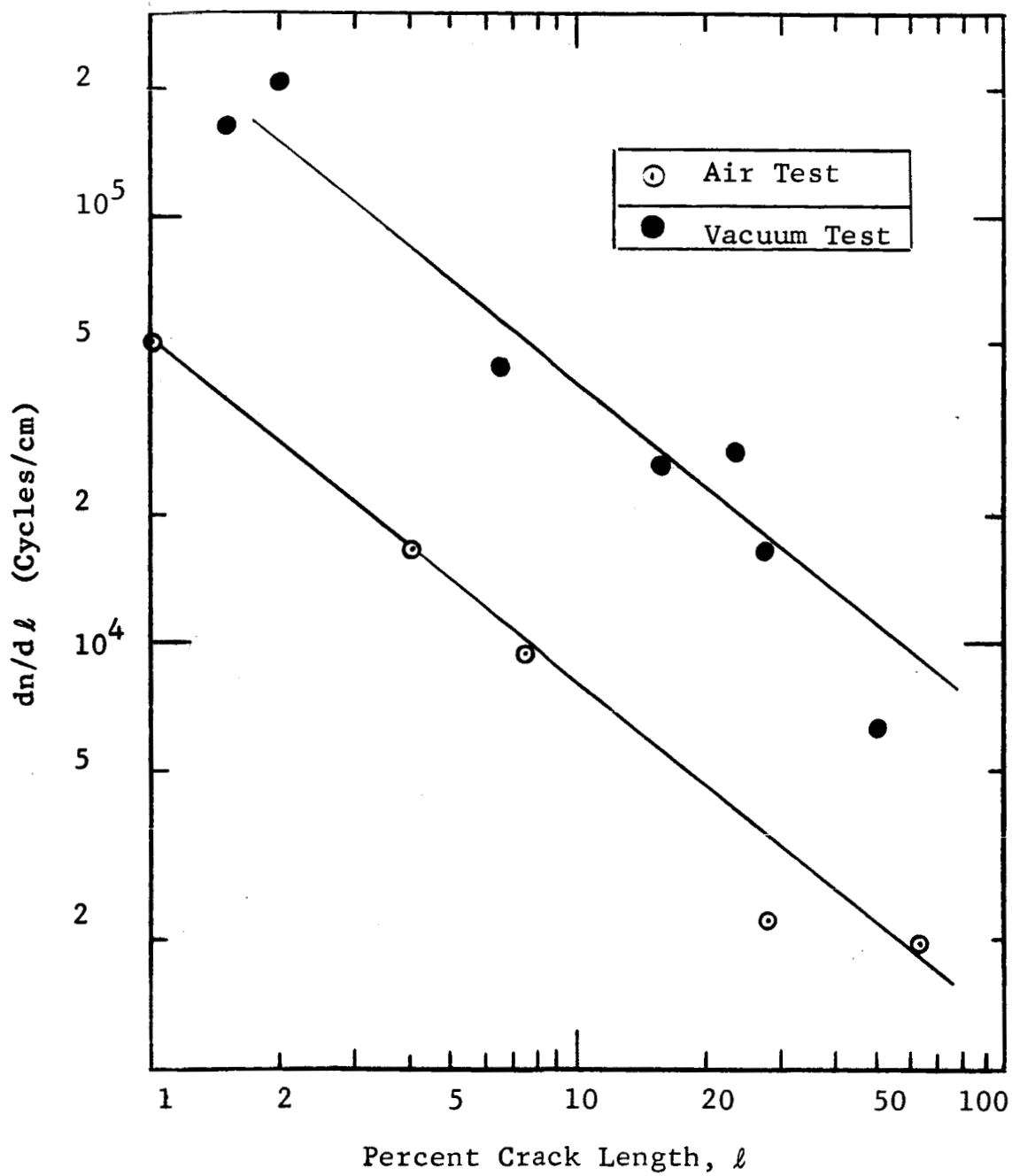


Fig. 13

CYCLIC CRACK PROPAGATION RATE VS. CRACK LENGTH

1.2×10^5 and 2.0×10^5 in air and vacuum, respectively. The estimated value of N_I for this strain amplitude from Equation (11) was about 2×10^5 cycles.

It has been postulated by May¹⁴ that fatigue crack nucleation takes place due to the concentration of slip in surface intrusions previously formed on the specimen. May determined that 1.3×10^5 cycles of stress would be necessary to produce a crack nucleus. The correspondence between this theoretically derived value and the present experimental results would seem to confirm the validity of the approach, although the metallurgical observations presented later in this report appear to place the actual details of the mechanism in question.

Figure 14 illustrates the change in the crack growth rate that takes place when the environmental test gas pressure is changed during a test. It is interesting to note that the instantaneous rate change which occurs when the test pressure is increased is not apparent when the test pressure is lowered from atmospheric pressure to 10^{-7} Torr. It can be seen that a definite incubation period occurs before the high propagation rate typical of an air environment diminishes to the low propagation value observed in vacuum. This phenomena may be attributed to a reaction occurring between the freshly exposed aluminum and residual oxygen that is trapped at the crack tip. This limited reaction prevents the crack growth rate from immediately changing to that value normally observed in a vacuum environment.

Frequency effects. — The experimental portion of the work reported in the previous sections was carried out by stressing the specimens at two different frequencies, 25 and 50 cycles per second. It was noted that a fatigue crack invariably propagated at a slower rate through specimens stressed at the higher frequency. Examples of this type of behavior are shown in Figures 15 through 17. In all these cases, the crack propagates more slowly in the specimen tested at the higher frequency regardless of the environmental testing conditions.

Metallurgical investigation. — The surface of a typical specimen fatigued to fracture in air is shown in Figure 18. The areas surrounding the dominant fatigue crack are seen to contain numerous surface markings that have the appearance of small, undeveloped cracks. The surface of a similar specimen stressed in vacuum, shown in Figure 19, contains similar markings that are more numerous and more developed. Figures 20 (a) and

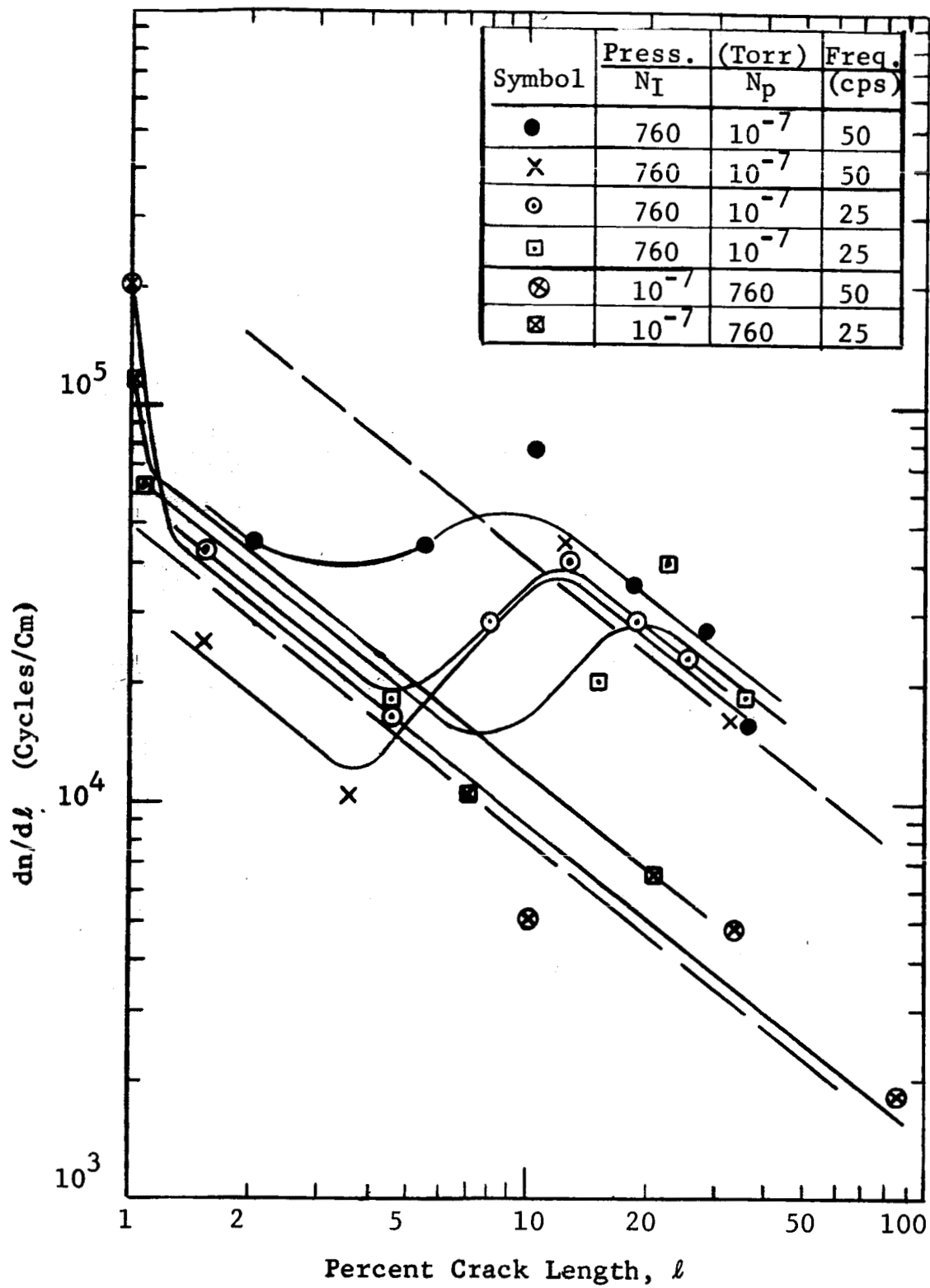


Fig. 14

THE EFFECT OF TEST INTERRUPTION
ON THE CYCLIC CRACK PROPAGATION RATE

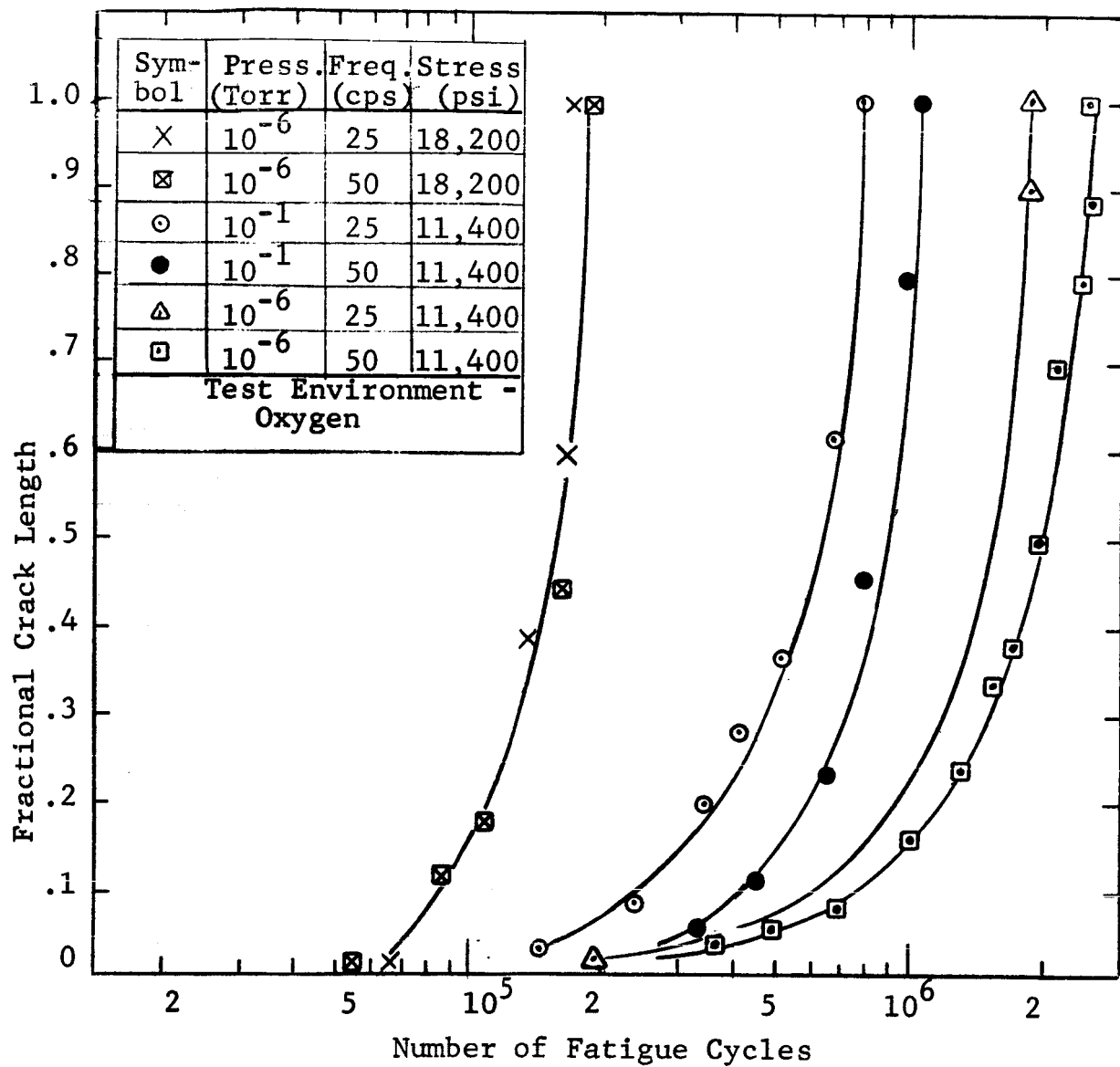


Fig. 15

THE EFFECT OF FREQUENCY ON CRACK PROPAGATION
IN OXYGEN ENVIRONMENT

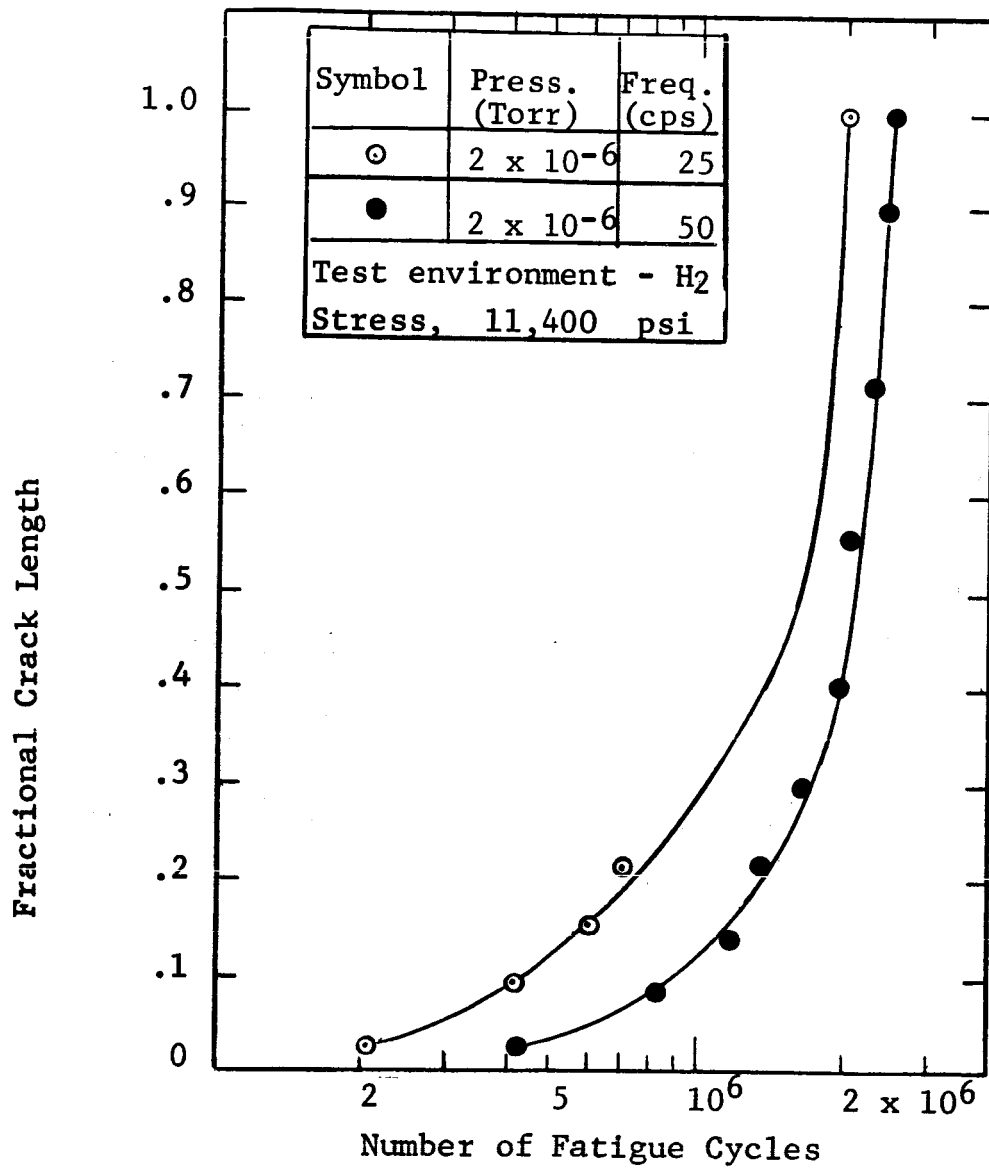
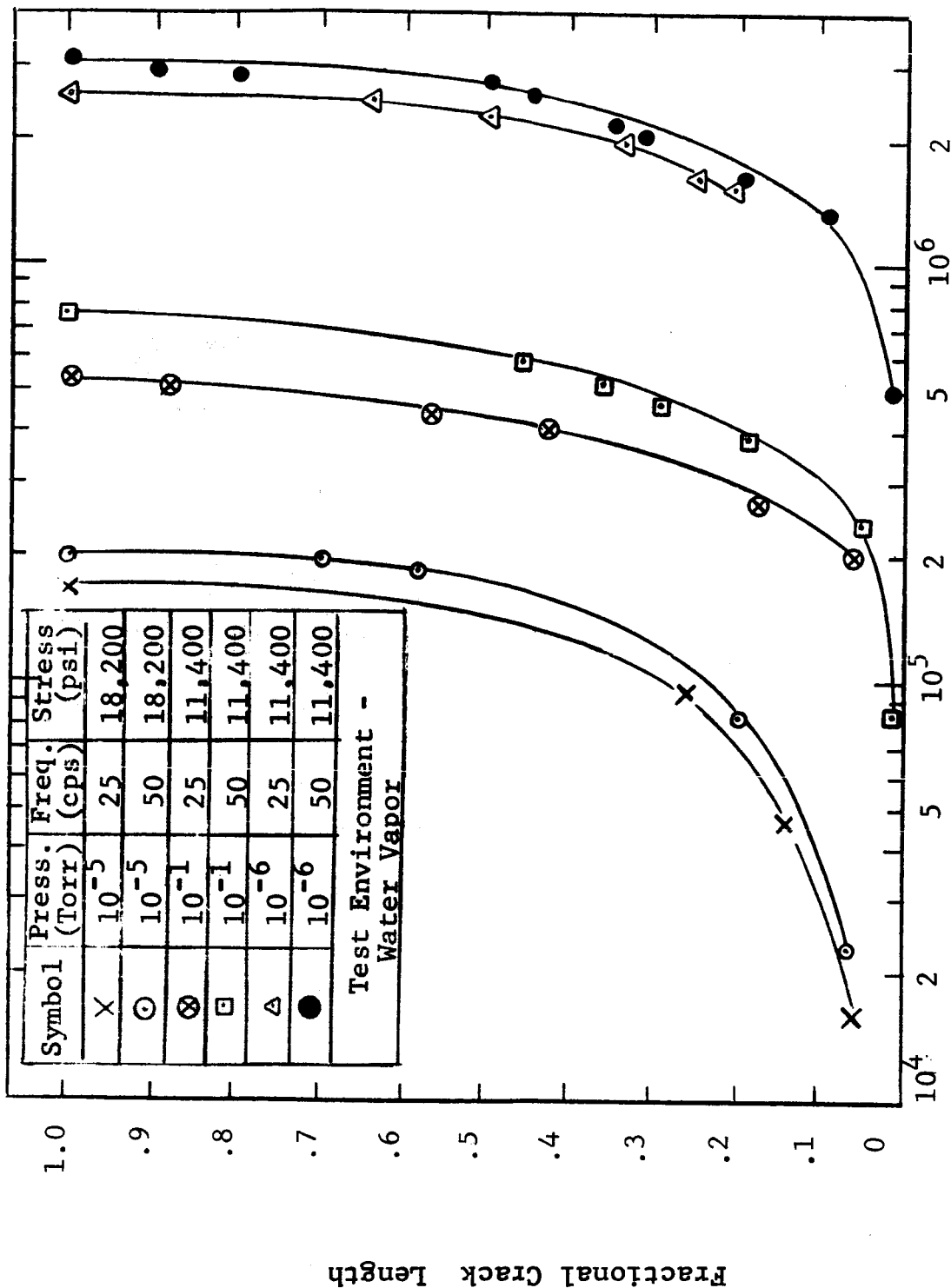


Fig. 16

THE EFFECT OF FREQUENCY ON CRACK PROPAGATION
IN HYDROGEN ENVIRONMENT



THE EFFECT OF FREQUENCY ON CRACK PROPAGATION
IN WATER VAPOR ENVIRONMENT
Fig. 17

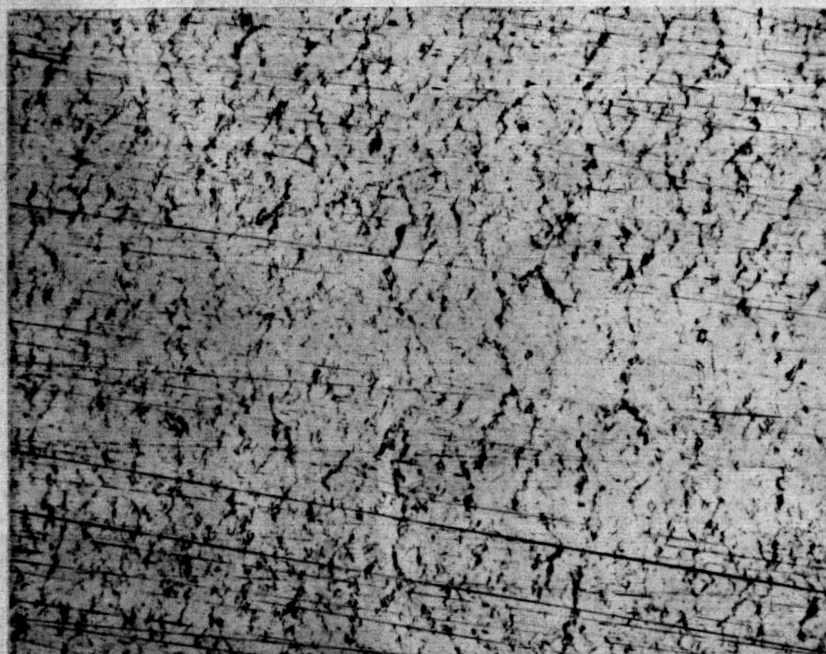


Fig. 18

SURFACE OF ALUMINUM SPECIMEN
CYCLED TO FRACTURE IN AIR. (25x)

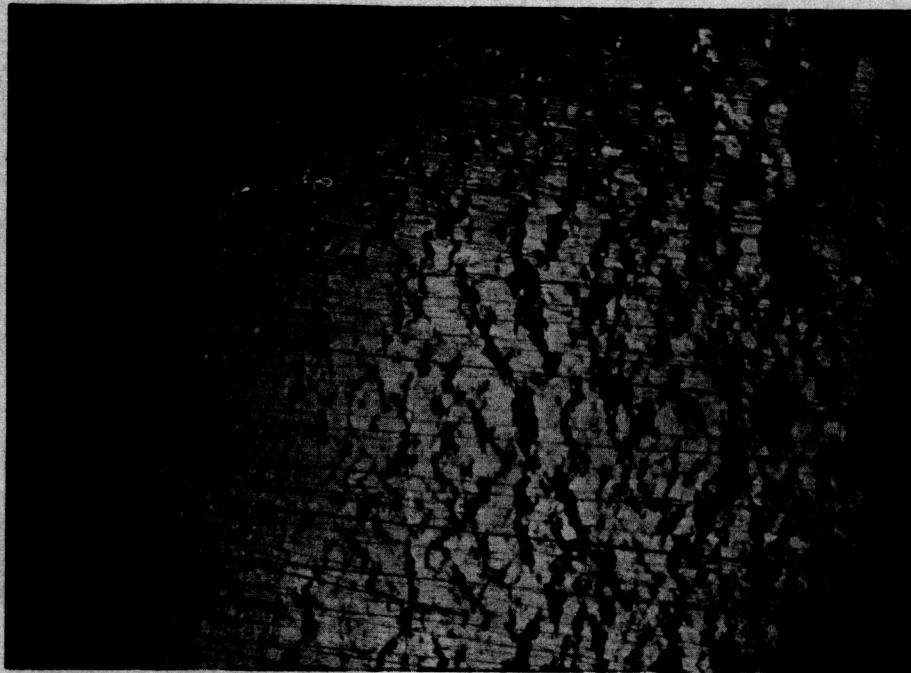
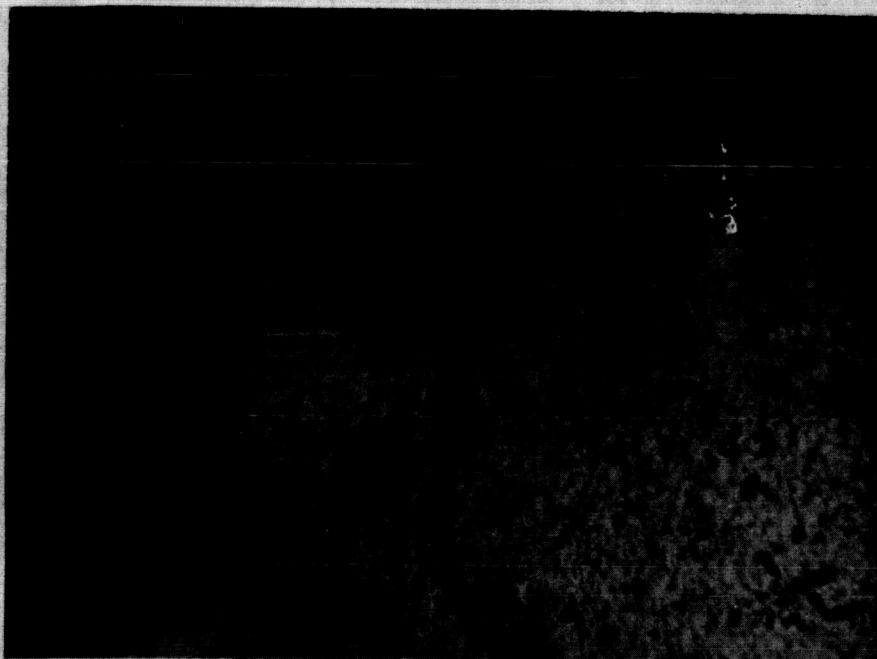
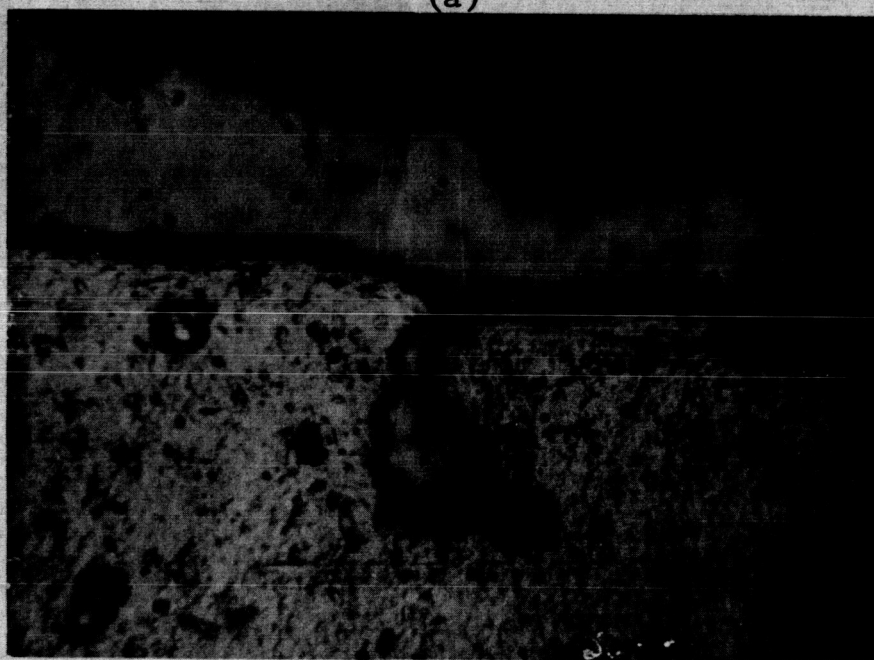


Fig. 19

SURFACE OF ALUMINUM SPECIMEN
CYCLED TO FRACTURE AT A
PRESSURE OF 10^{-7} TORR. (25x)



(a)



(b)

Fig. 20

SECTIONS THROUGH ALUMINUM SPECIMENS
SUBJECTED TO A FATIGUE STRESS AT A
PRESSURE OF 10^{-7} TORR. (SURFACE
COPPER PLATED) (1500x)

(b), taken from a cross section of a vacuum fatigue specimen, indicate the depth of these cracks to be about 10^{-3} inches.

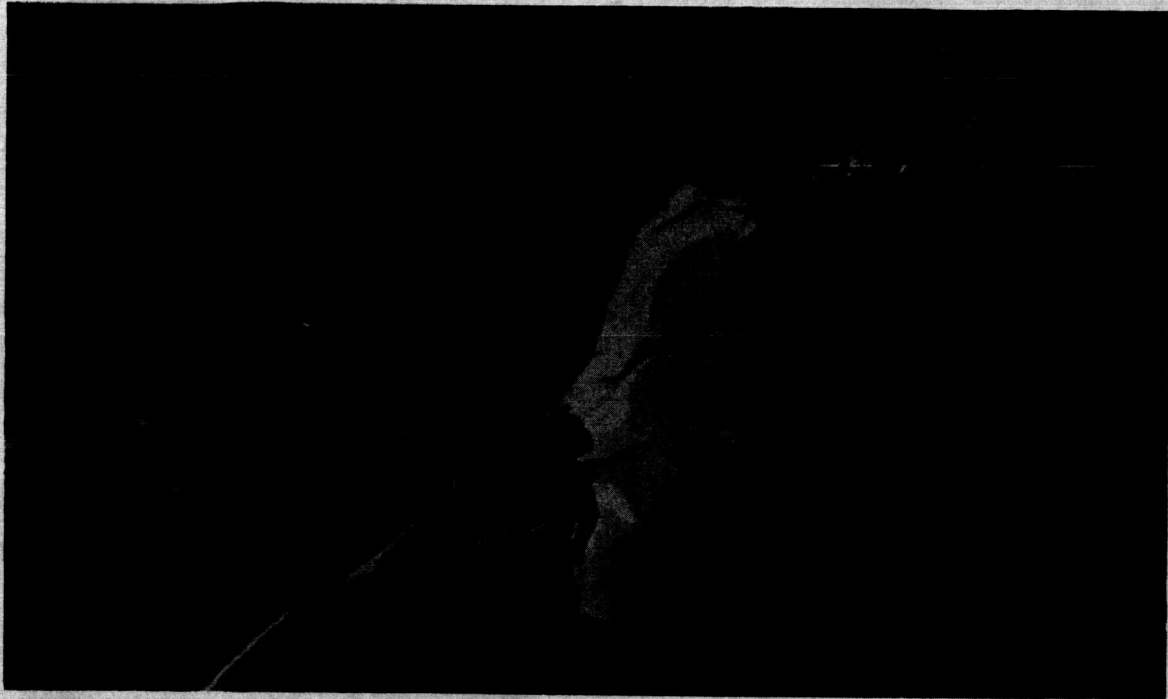
The reason for the more pronounced markings observed in vacuum is not known; however, it has been shown that a fatigue crack propagates more slowly across a specimen stressed at low pressures. The critical surface condition of stress remains uniform for an extended period of time and deformation is not concentrated at any specific crack tip. The crack nuclei formed in vacuum develop to a later stage before coalescence forms a dominant crack which rapidly propagates.

A clue to the small environmental dependence of the rate of crack nucleation is furnished by Figure 21. An electron microscopical technique has been used to magnify the surface of the crack nuclei; it can be seen that the surface of aluminum is lifting, presumably as a result of some subsurface damage. Environmental effects are naturally greatest at the surface, thus subsurface nucleation would be expected to show little dependence on pressure. A surprising feature of fatigue tests carried out in bending on half hard aluminum is the absence of surface slip markings. The surface of the crack nuclei shown in Figures 22 (a) and (b) illustrate this phenomena. It can be seen that these crack nuclei have formed without the appearance of surface slip lines; indeed the topographical features present in these photographs again suggest that some subsurface mechanism is responsible for crack nuclei formation.

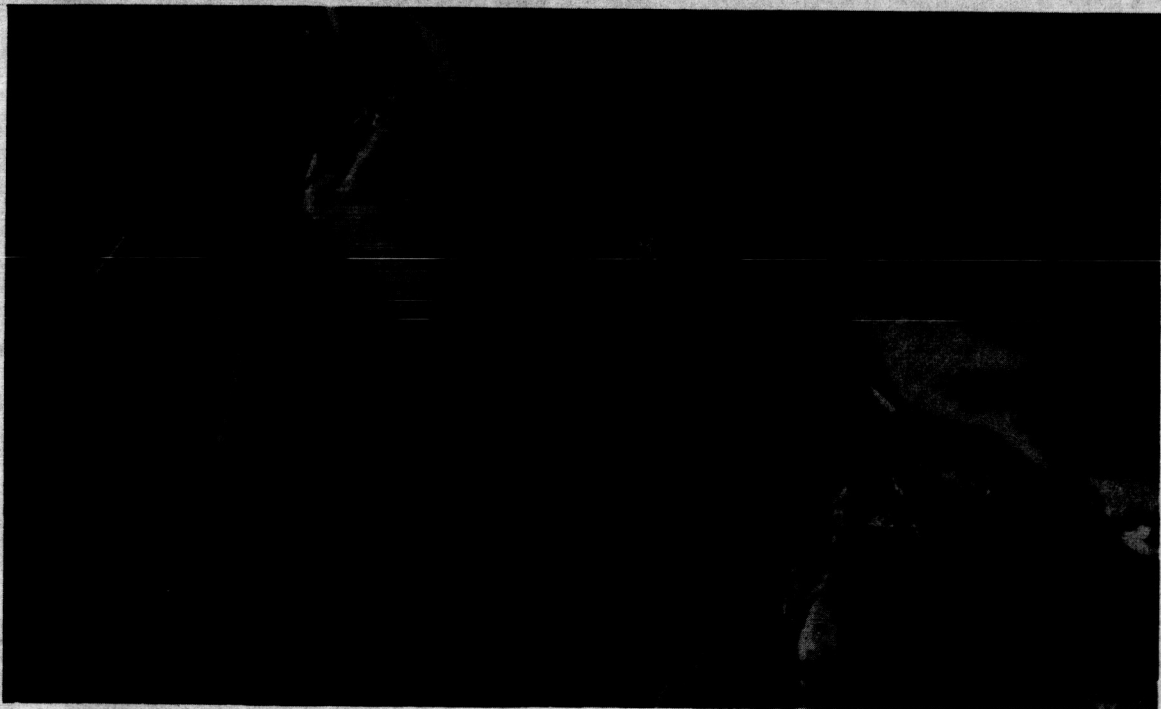
Aluminum is a high stacking fault energy material; hence, any moving dislocation would be expected to cross slip easily in such a way as to form an interacting network of subgrain boundaries. The nuclei of subgrains are presumably already present in the half hard aluminum used in this investigation; little dislocation movement is needed to perfect them before they become progressively mis-oriented with respect to each other. In this connection, experiments, using strain gauges, carried out in previous research ⁹ indicated that the hardness of half hard aluminum remained constant during fatigue tests; thus any dislocation generation was balanced by an apparent annihilation process, presumably subgrain formation. It may be surmised that the subgrain boundaries are regions of weakness which provide an easy crack propagation path. Figure 23 shows a fatigue crack, which did not lead to final fracture; this crack is observed to delineate many subgrain boundaries, the size of which vary in diameter from 0.5 to 3×10^{-4} cm.



Fig. 21
ELECTRON MICROGRAPH SHOWING THE FORMATION
OF A CRACK BY SURFACE UPHEAVAL (18,800x)



(a)



(b)

Fig. 22

ELECTRON MICROGRAPH OF ALUMINUM FATIGUE
SPECIMEN SURFACE SHOWING CRACK NUCLEI (18,800x)

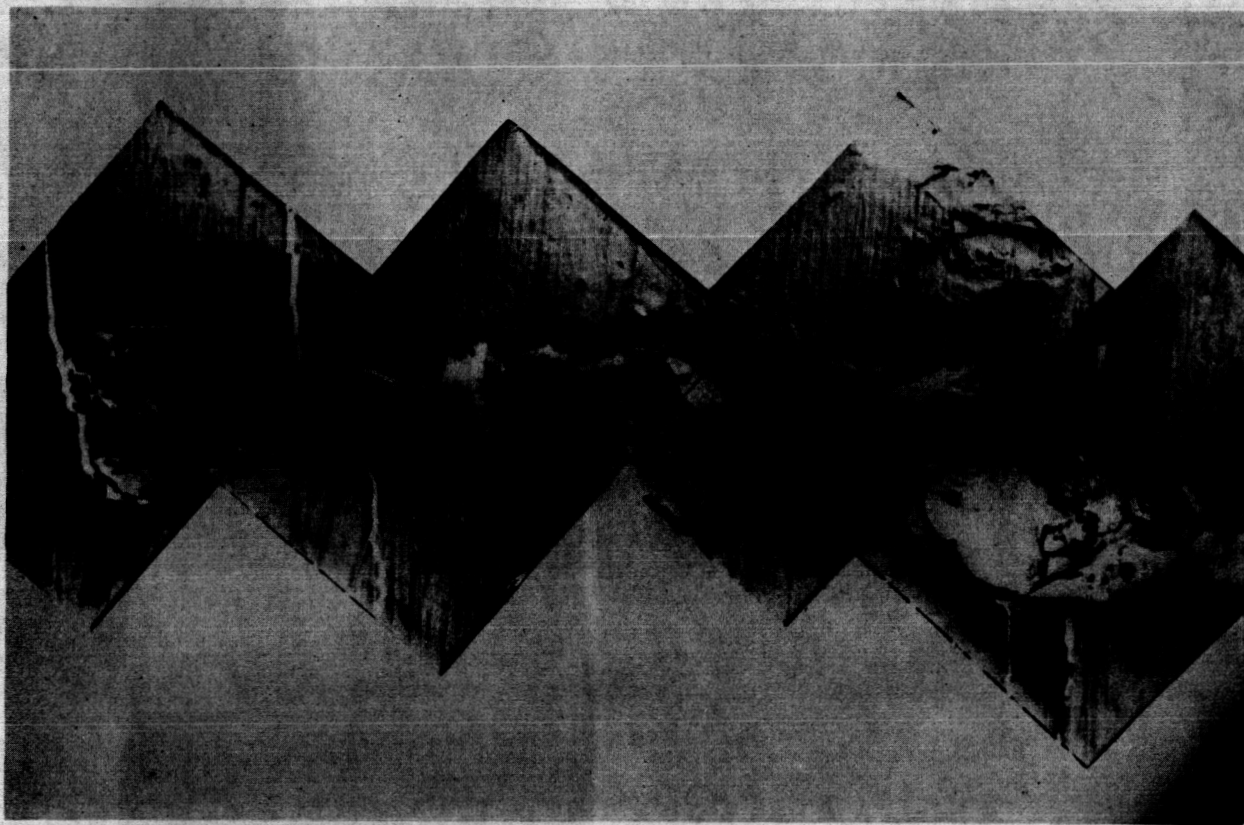


Fig. 23
COMPOSITE ELECTRON MICROGRAPH SHOWING
TYPICAL SURFACE FATIGUE CRACK. (5340x)

Examination of the fatigue crack fracture surface shows that the growth of the final crack takes place by many mechanisms. The "ripple" markings typical of fatigue crack propagation are shown in Figure 24; the main crack front in this case consisted of several smaller fronts proceeding on different planes in the metal. Figure 25 shows similar ripple markings at higher magnification. The distance between the markings defines the length of crack extension per cycle, in this case 2.5×10^{-5} cm/cycle. It is to be noted from this figure that appreciable tearing takes place between areas covered by ripples. It is surmised, therefore, that each crack is nucleated by some subsurface mechanism and is propagated, presumably by the blunting and sharpening of the crack tip as proposed by Laird and Smith¹⁵. It is expected that gas penetrating the crack reacts with the newly exposed metal and prevents the crack from rewelding providing the partial pressure of oxygen is high enough. The region between each embryo crack then may fracture by actual tearing of the metal.

Phase II

Extreme high vacuum fatigue tests. — Fatigue tests of 1100 aluminum were conducted in the XHV system after thermal outgassing to 150°C followed by cryogenic pumping. The specimens were maintained at 15 to 20°C by a water heating jacket while the cryoshield temperature was lowered to 12 to 20 °K. Initial vacuum levels in the range 1 to 5×10^{-11} Torr were obtained before fatigue operation.

With excitation of the vibrator mechanism, the pressure level was observed to rise rapidly to the range 3×10^{-10} to 2×10^{-9} Torr due to additional degassing of the specimens under vibration. After a short time increment, the pressure level reached a peak and thereafter decreased steadily throughout the remainder of the test. The initial portion of the indicated pressure-time histories of representative fatigue tests are presented in Figure 26. It is evident that a measurable amount of adsorbed gas on the specimen surfaces was given off with the alternating stress application. With continued stressing, the indicated pressure steadily decreased to approximately the initial value.

The results of fatigue tests carried out at 100 cps in unit atmosphere and at vacuum levels generally below 1×10^{-10} Torr are compared in Figure 27, in which the mean total fracture life band values indicate the spread in results for each group of eight simultaneously stressed specimens. The variation in fatigue life values are generally less than 40 percent. It is

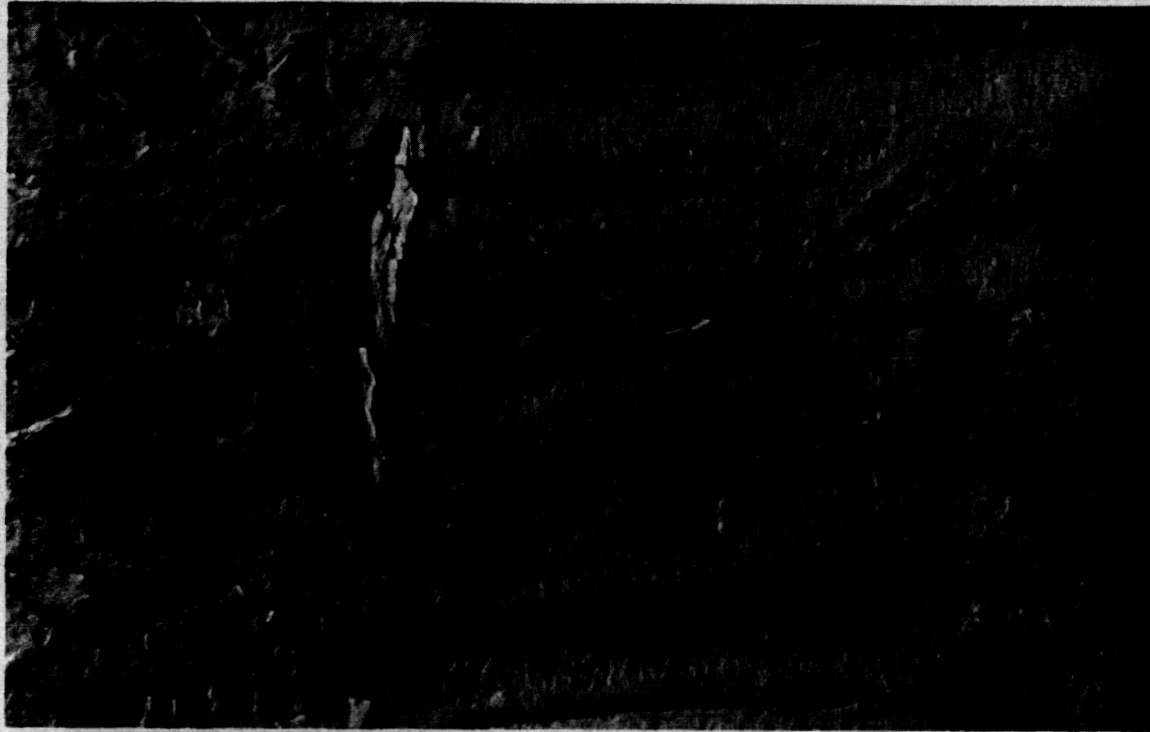


Fig. 24
FRACTURE SURFACE OF ALUMINUM FATIGUE
SPECIMEN SHOWING TYPICAL CRACK PROPAGATION
RIPPLES. (10,500x)

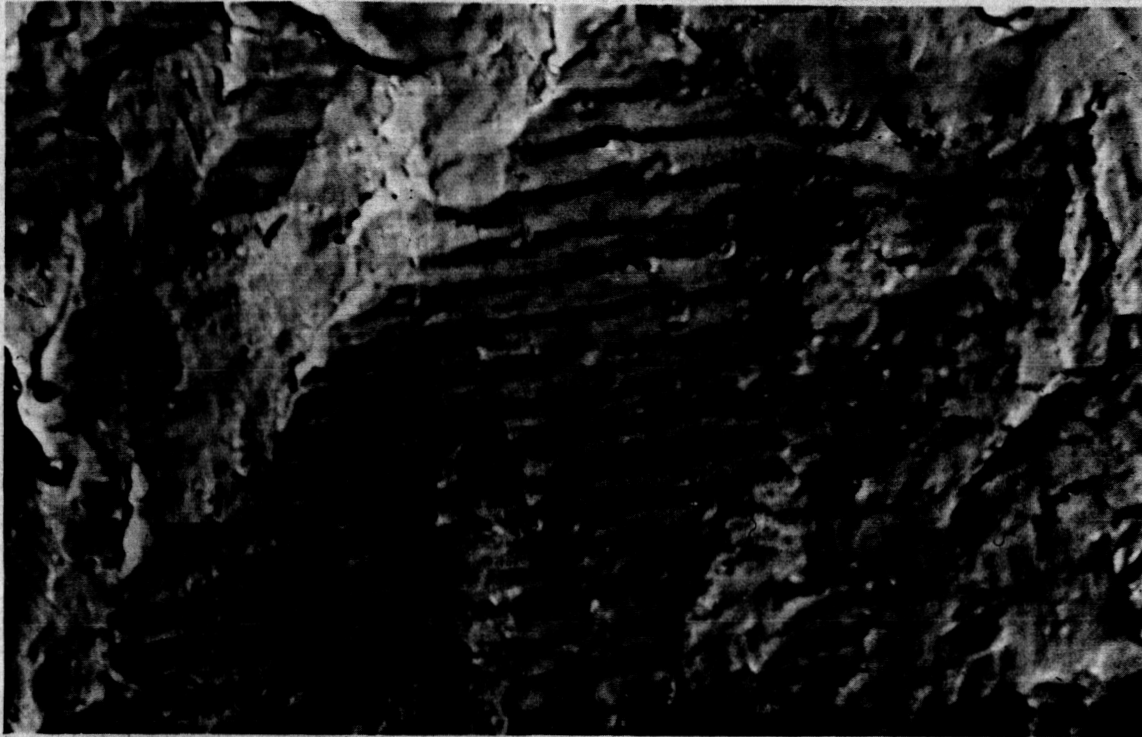


Fig. 25
HIGH MAGNIFICATION ELECTRON FRACTOGRAPH
SHOWING FATIGUE RIPPLES. (18,500x)

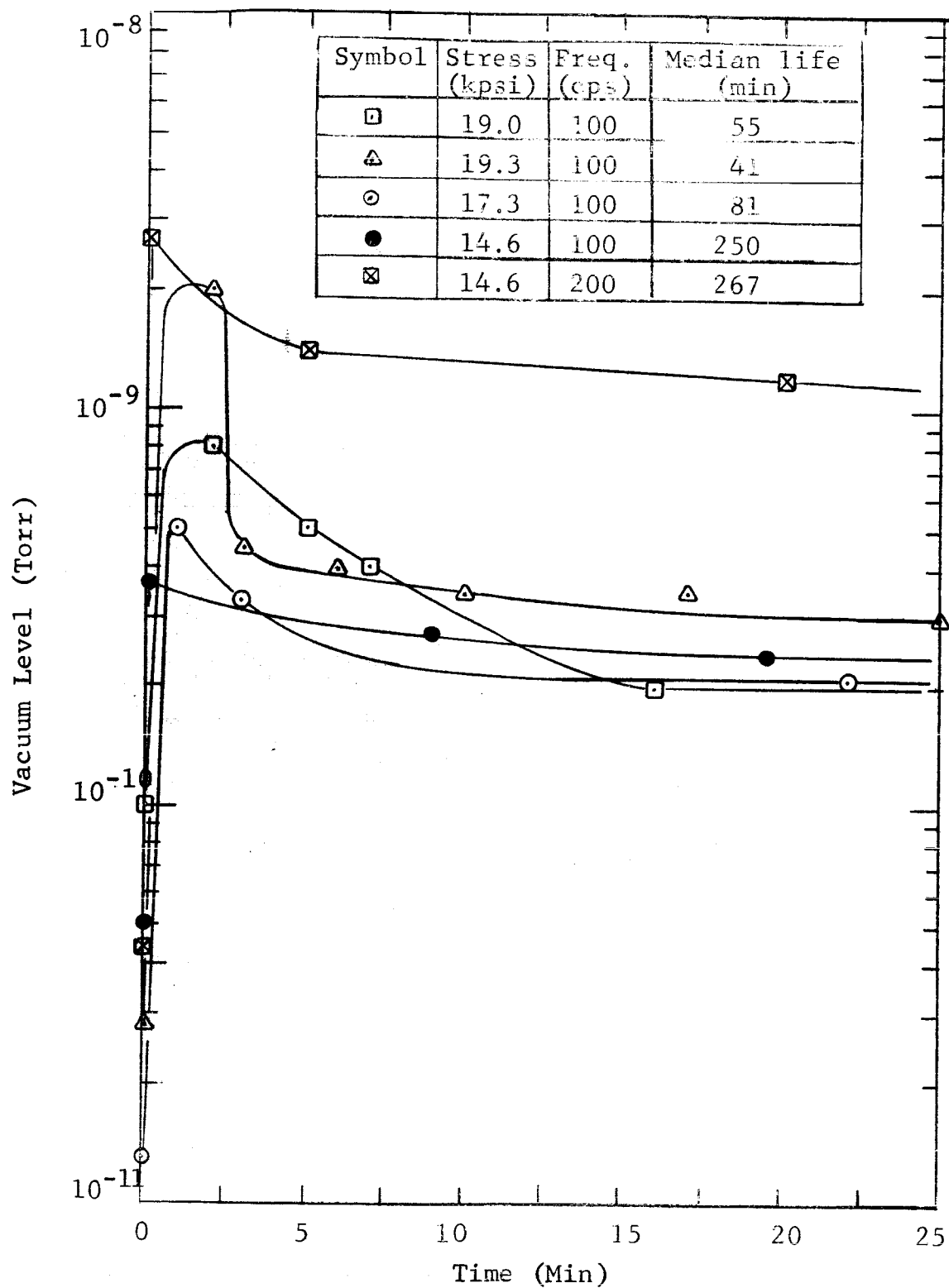


Fig. 26

PRESSURE VS. TIME DURING FATIGUE TEST

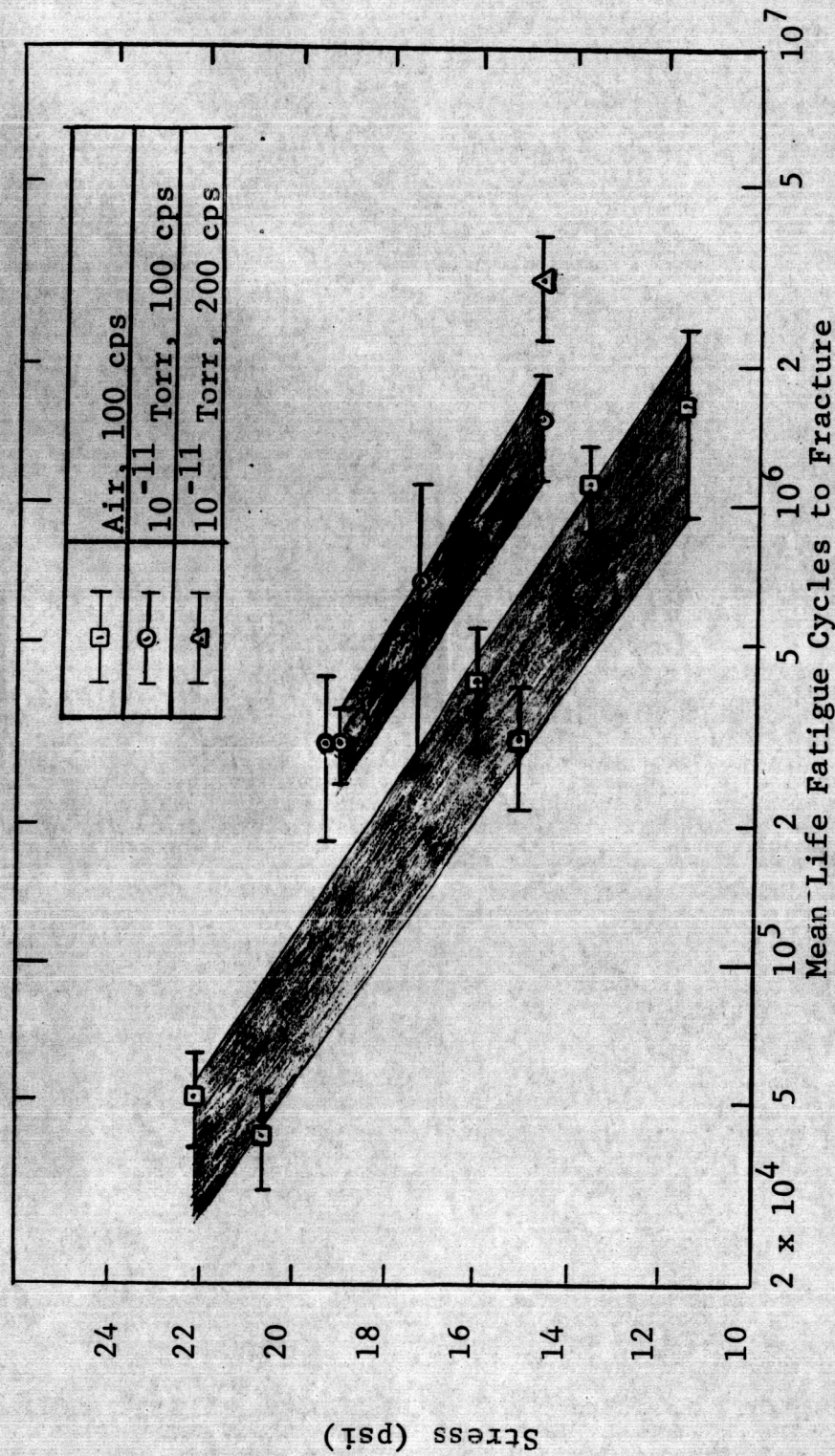


Fig. 27

AIR AND VACUUM S-N CURVES FOR 1100H14 ALUMINUM

readily apparent that the S-N band obtained in the vacuum tests was substantially displaced to the right compared to the band of values resulting from the air tests. The increase in fatigue life in the vacuum environment was in good agreement with the experimental studies carried out at higher pressure levels.

Analysis of the experimental data reported in Phase I tests showed that the increase in the fatigue resistance to fracture in a vacuum of 2×10^{-7} Torr was about 3 times the atmospheric value for a surface stress amplitude of 18,200 psi. The data at the 7×10^{-11} Torr level for an equivalent stress also show an improvement factor in vacuum remains essentially constant for all pressures below 10^{-7} Torr in the case of aluminum fatigued at reverse loading rates above 25 cps.

Frequency effects. — The effect of cyclic stress frequency in vacuum was examined by comparing the fatigue behavior of aluminum at 14,600 psi surface stress corresponding to a constant surface strain amplitude of ± 0.00146 for both 100 and 200 cps reverse bending rates. The results are also indicated in Figure 27. It is apparent that increasing the stress frequency by a factor of 2 resulted in similar increase in the mean number of cycles to fracture; 1.55×10^6 to 3.13×10^6 cycles. The increase in fatigue resistance with frequency can be attributed to the equivalence of the time rate of crack extension at pressure levels well below the critical transition zone.

The time required for contamination of a fatigue crack by oxygen or water vapor adsorption can be derived from Equation (3):

$$t_a = \frac{1}{K} \frac{(MT)^{1/2}}{p_i} \quad \text{sec/cm} \quad (12)$$

where K is given in Equation (4). Considering oxygen as the adsorbing molecule and assuming $po_2 = P/5$, then

$$t_a \simeq 5 \times 10^{10} \quad \text{sec/cm} \quad (13)$$

for the values $P = 1 \times 10^{-10}$ Torr, $T = 291^\circ\text{K}$, $M = 32$, $A = 1.0 \times 10^{-15} \text{ cm}^2$ and $l/r = 10^3$. Since the actual time

required to propagate the crack was about 1.4×10^4 sec through the specimen half-depth of about 0.10 cm, the required equivalent crack growth time per unit length of extension was only about 1.4×10^5 sec/cm. It is apparent that the time rate of crack extension far exceeded the exposure time required for crack contamination. In the indicated 10^{-10} Torr pressure range, the alternating stress frequency would have to be decreased by a factor 10^5 before a measurable contamination effect would be expected.

Comparison of extreme high vacuum and intermediate vacuum results. — One of the major goals of the current investigation was to extend the range of observations of the vacuum environment on fatigue behavior to pressure levels below 10^{-10} Torr approximating the conditions in deep space and to compare these results with observations made at intermediate pressure levels in the range 10^{-3} to 10^{-8} Torr. Representative composite results from Phase I and Phase II studies are presented in Figure 28 in which the normalized average time required for fatigue failure at a constant surface strain amplitude of ± 0.0012 is plotted over the entire pressure range covered in this work. The data given for pressure levels above 10^{-7} Torr were taken from fatigue tests run at 25 cps alternating stress rates; the data for the 5×10^{-11} Torr level were taken from 100 cps tests.

It is apparent that the average time required to propagate a fatigue crack from nucleation to failure approached a stable limit as the pressure was decreased below 10^{-7} Torr. A further pressure decrease below 10^{-11} Torr, would not be expected to significantly change the fatigue resistance. With increase in pressure above 10^{-7} Torr, the fracture speed was noticeably increased particularly in the range 10^{-2} to 10^{-5} Torr. This change in the fracture time can be attributed to oxide contamination of the fatigue crack. At pressure levels above 10^{-1} Torr, the rate of oxygen reaction at the crack tip may be expected to be so rapid that the fatigue properties are insensitive to further increases in the environmental gas pressure.

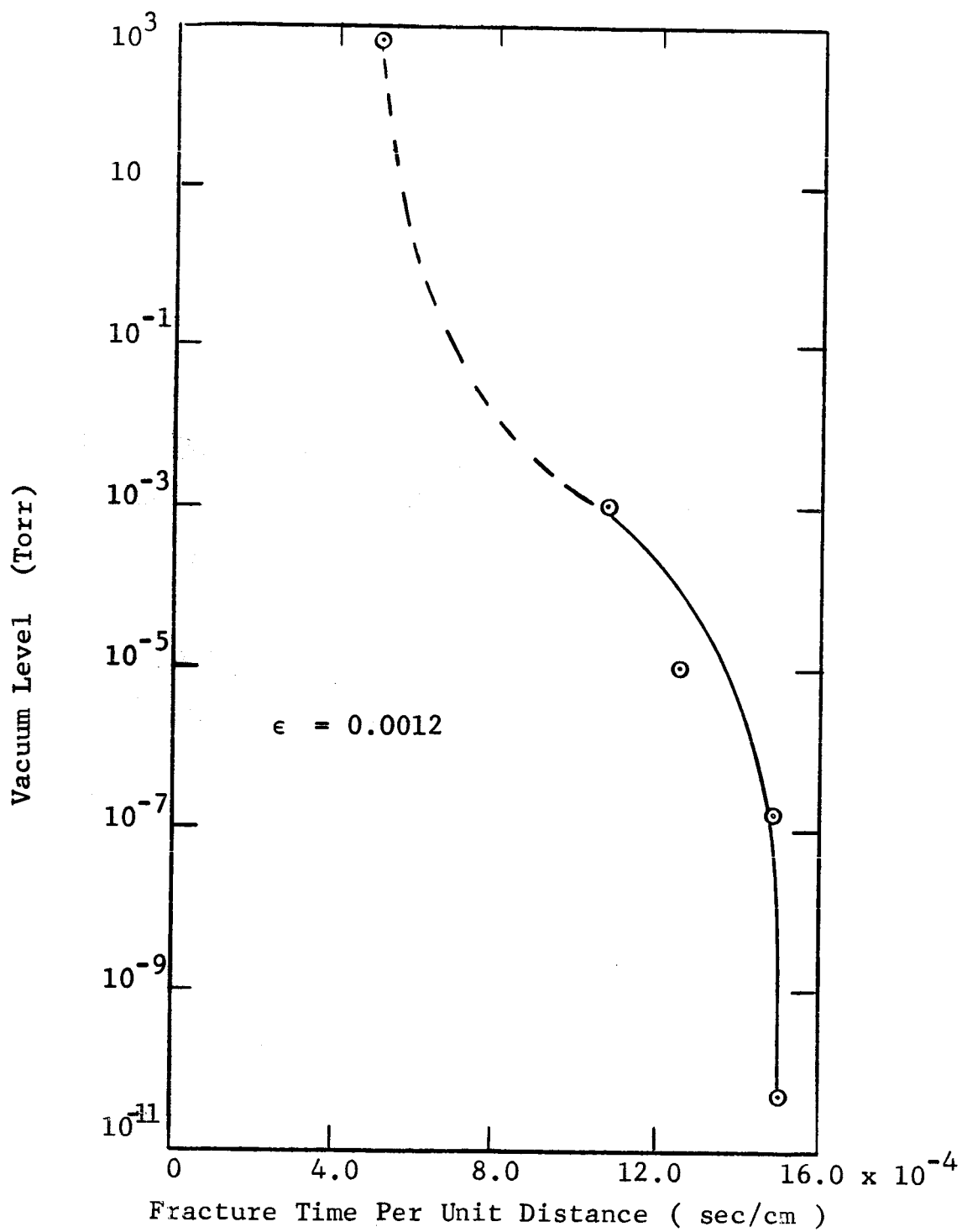


Fig. 28

RECIPROCAL OF THE FATIGUE CRACK EXTENSION RATE VS VACUUM LEVEL

CONCLUSIONS

From the results of the present work, the following conclusions may be stated:

(1) The oxide, crack contamination hypothesis advanced in previous work under Contract No. NASw-962 appears to be supported by extended investigation. Specifically, the increase of the fatigue transition pressure zone with temperature for aluminum can be accounted for by changes in the pressure dependence of the oxygen or water vapor adsorption rate and the rate of crack extension with temperature.

(2) Fatigue tests interrupted after nucleation of a visible crack and continued at different pressure values have demonstrated that the crack nucleation phase of the fatigue process was largely insensitive to the surrounding gas pressure level. On the other hand, the rate of crack growth was influenced by the gas pressure; an increase of pressure raising the growth rate while a drop in pressure retarded the rate.

(3) Fatigue experiments run in different residual gas media showed that oxygen adsorption either from oxygen gas molecules or from dissociated water vapor molecules was the most probable cause for fatigue life reduction at standard pressure levels. Oxygen-free hydrogen gas was clearly not as detrimental to the fatigue properties as either O_2 or H_2O gas.

(4) Fatigue tests run at extremely low pressures below 1×10^{-10} Torr showed little further fatigue life improvement over the experimental results at higher pressures in the range 10^{-5} to 10^{-7} Torr. The fatigue life stability at pressures below the transition zone may be attributed to the lessening effect of oxygen adsorption in enhancing crack propagation and the predominance of stress intensity and microstructural effects in determining the rate of crack growth.

(5) Fatigue tests at less than 1×10^{-10} Torr showed that, in agreement with prior results at intermediate pressures, the number of cycles required for fatigue failure increased substantially with an increase in the alternating stress frequency. Specifically, increasing the frequency by a factor of two resulted in doubling the fatigue life. Comparable results at lower vacuum levels showed that approximately 50 percent increase in the cyclic life could be expected with an equivalent change in frequency. The cyclic dependence on rate of stress application may be attributed to the importance of the exposure

time at any pressure level. When the rate of crack growth under oxygen-free conditions is large enough to cause fracture in less time than that required for adsorption and contamination, variation in the frequency stressing will generally not affect the time rate of extension along the fracture path.

FUTURE WORK

Although the effect of residual gas atmospheres on the fatigue behavior of metals is an extremely broad field, the following specific suggestions are outlined for extending the work of the current investigation on the fatigue properties of aluminum in vacuum.

(1) Since crack exposure time is apparently a major factor controlling the fatigue crack growth, tests should be run with a variation in the exposure time by adjusting the ratio of maximum and mean surface bending stresses. By adjusting the mean stress from zero to one-half the maximum stress, the exposure time per stress cycle can be varied from 0.5 to 1.0.

(2) In an oxygen-free gas environment, the fatigue propagation mechanism will be dominated by stress and microstructural conditions. Observations of the basic fracture process by electron fractography and transmission electron microscopy techniques will be of interest. In addition, comparative studies should be made under vacuum and standard atmospheric conditions in order to detect possible changes in the mechanism of crack growth indicative of oxygen reaction.

(3) Substructural details such as subgrain size may play an important role in crack propagation. In particular, the possible relation of a critical subgrain size to the fatigue endurance limit should be examined.

(4) The current results show that the cyclic life to fracture in vacuum is strongly dependent on the cyclic frequency or number of stress applications per unit time. An investigation of the variation of the number of cycles to fracture with stress frequency, stress amplitude and pressure level should be made over a wide range of values to examine this effect in more detail.

REFERENCES

1. Hordon, M.J.: Fatigue Behavior of Aluminum in Vacuum. *Acta Met.*, vol. 14, 1966, p. 1173.
2. Wright, M.A.; and Hordon, M.J.: Temperature Dependence of Fatigue Transition Pressure. *Acta Met.*, vol. 15 (to be published), 1967.
3. Jastrow, R.: Lunar and Terrestrial Atmospheres, Adv. in *Aero Science*, vol. 5, Plenum Press, Inc., New York, 1960.
4. Gough, H.S.; and Sopwith, D.G.: Atmospheric Action as a Factor in Fatigue of Metals. *J. Inst. Met. (Lond.)*, vol. 49, 1932, p. 93.
5. Gough, H.S.; and Sopwith, D.G.: Some Further Experiments On Atmospheric Action in Fatigue. *J. Inst. Met. (Lond.)*, vol. 56, 1935, p.55.
6. Snowden, K.U.: The Effect of Atmosphere on the Fatigue of Lead. *Acta Met.*, vol. 12, March 1964, p. 295.
7. Wadsworth, N.J.: The Effect of Environment on Metal Fatigue. Ed. Rassiviler, G.M., and Grube, W.L.: *Internal Stresses and Fatigue in Metals*. Elsevier Amsterdam, 1959, p.382.
8. Ham, J.L.; and Reichenbach, G.S.: Fatigue Testing of Aluminum in Vacuum. *Symposium on Materials for Aircraft, Missiles and Space Vehicles*, Special Tech. Pub. No. 345, Amer. Soc. for Test. Mat., 1962.
9. Hordon, M.J.; and Reed, M.E.: Study of the Mechanism of Atmospheric Interaction with the Fatigue of Metals. NASA CR-68036, 1965.
10. Lyman, T., ed.: *Metals Handbook*. Vol. 1, Eighth ed., Amer. Soc. Metals, Novelty, Ohio, c. 1961, p. 936.
11. Snowden, K.U.: Effect of Gaseous Environment on Crack Propagation. *J. App. Phys.*, vol. 34, 1963, p. 3150.
12. McCammon, R.D.; and Rosenberg, H.M.: The Fatigue and Ultimate Tensile Strengths of Metals Between 4.2 and 293 °K. *Proc. Roy. Soc. (Lond.)*, vol. 242, Ser. A, 1957, p. 203.

13. Youden, W.J.: Statistical Methods for Chemists. John Wiley and Sons, Inc., 1951, p. 24.
14. May, A.N.: A Model of Metal Fatigue. Nature, vol.185, 1960, p. 303.
15. Laird, C; and Smith, G.C.: Crack Propagation in High Stress Fatigue. Phil Mag. vol 7, 1962, p. 847.